Published in final edited form as:
Cancer Biol Ther. 2008 October ; 7(10): 1648–1662.

Vorinostat and sorafenib increase ER stress, autophagy and apoptosis via ceramide-dependent CD95 and PERK activation

Margaret A. Park[1], **Guo Zhang**[1], **Aditi Pandya Martin**[1], **Hossein Hamed**[1], **Clint Mitchell**[1], **Philip B. Hylemon**[6], **Martin Graf**[3], **Mohamed Rahmani**[1,2], **Kevin Ryan**[9], **Xiang Liu**[8], **Sarah Spiegel**[1], **James Norris**[8], **Paul B. Fisher**[5,7], **Steven Grant**[1,2,7], and **Paul Dent**[1,4,7,*]

1*Department of Biochemistry, Virginia Commonwealth University, 401 College St., Richmond, VA 23298*

2*Department of Medicine, Virginia Commonwealth University, 401 College St., Richmond, VA 23298*

3*Department of Neurosurgery, Virginia Commonwealth University, 401 College St., Richmond, VA 23298*

4*Department of Radiation Oncology, Virginia Commonwealth University, 401 College St., Richmond, VA 23298*

5*Department of Human Genetics, Virginia Commonwealth University, 401 College St., Richmond, VA 23298*

6*Department of Microbiology and Immunology, Virginia Commonwealth University, 401 College St., Richmond, VA 23298*

7*Institute for Molecular Medicine, Virginia Commonwealth University, 401 College St., Richmond, VA 23298*

8*Department of Microbiology and Immunology, Medical University of South Carolina, 86 Jonathan Lucas Street, Charleston, SC 29425*

9*The Beatson Institute for Cancer, Research Garscube Estate, Switchback Road, Glasgow, G61 1BD, UK*

Abstract

We recently noted that low doses of sorafenib and vorinostat interact in a synergistic fashion to kill carcinoma cells by activating CD95, and this drug combination is entering phase I trials. The present studies mechanistically extended our initial observations. Low doses of sorafenib and vorinostat, but not the individual agents, caused an acidic sphingomyelinase and fumonisin B1-dependent increase in CD95 surface levels and CD95 association with caspase 8. Knock down of CD95 or FADD expression reduced sorafenib/vorinostat lethality. Signaling by CD95 caused PERK activation that was responsible for both promoting caspase 8 association with CD95 and for increased eIF2α phosphorylation; suppression of eIF2α function abolished drug combination lethality. Cell killing was paralleled by PERK- and eIF2α-dependent lowering of c-FLIP-s protein levels and over-expression of c-FLIP-s maintained cell viability. In a CD95-, FADD- and PERK-dependent fashion, sorafenib and vorinostat increased expression of ATG5 that was responsible for enhanced autophagy. Expression of PDGFRβ and FLT3 were essential for high dose single agent sorafenib treatment to promote autophagy. Suppression of PERK function reduced sorafenib and vorinostat lethality whereas suppression of ATG5 levels elevated sorafenib and vorinostat lethality. Over-expression of c-FLIP-s blocked apoptosis and enhanced drug-induced autophagy. Thus sorafenib and vorinostat promote ceramide-dependent CD95 activation followed by induction of multiple downstream survival regulatory signals: ceramide-CD95-PERK-FADD-pro-caspase 8 (death); ceramide-CD95-PERK-eIF2α -↓c-FLIP-s (death); ceramide-CD95-PERK-ATG5-autophagy (survival).

*Correspondence to: Paul Dent, Ph.D., Department of Biochemistry and Molecular Biology, 401 College Street, Massey Cancer Center, Room 280a, Box 980035, Virginia Commonwealth University, Richmond VA 23298-0035. Tel: 804 628 0861, Fax: 804 827 1309, pdent@vcu.edu

Keywords

Vorinostat; Sorafenib; CD95; c-FLIP-s; PDGFRβ; FLT3; autophagy; ceramide; cell death; ASMase

Introduction

In the United States, hepatoma, renal and pancreatic carcinomas have 5 year survival rates of less than 10%, less than 5% and of 5-10%, respectively.[1] Melanoma that has spread beyond the radial growth phase (≥ stage III) has a mean 5 year survival rate of >20%.[2] These statistics emphasize the need to develop novel therapies against these lethal malignancies.

The Raf / mitogen-activated protein kinase (MAPK) kinase 1/2 (MEK1/2) / extracellular signal-regulated kinase 1/2 (ERK1/2) pathway is frequently dysregulated in neoplastic transformation .[3-5] The MEK1/2-ERK1/2 module comprises, along with c-Jun NH_2-terminal kinase (JNK1/2) and p38 MAPK, members of the MAPK super-family. These kinases are involved in responses to diverse mitogens and environmental stresses and have also been implicated in cell survival processes. Activation of the ERK1/2 pathway is generally associated with cell survival whereas induction of JNK1/2 and p38 MAPK pathways generally signals apoptosis. Although the mechanisms by which ERK1/2 activation promote survival are not fully characterized, a number of anti-apoptotic effector proteins have been identified, including increased expression of anti-apoptotic proteins such as c-FLIP.[6-11] In view of the importance of the RAF-MEK1/2-ERK1/2 pathway in neoplastic cell survival, inhibitors have been developed that have entered clinical trials, including sorafenib (Bay 43-9006, Nexavar®; a Raf kinase inhibitor) and AZD6244 (a MEK1/2 inhibitor).[12, 13]

Sorafenib is a multi-kinase inhibitor that was originally developed as an inhibitor of Raf-1, but which was subsequently shown to inhibit multiple other kinases, including class III tyrosine kinase receptors such as platelet-derived growth factor, vascular endothelial growth factor receptors 1 and 2, c-Kit and FLT3.[14] Anti-tumor effects of sorafenib in renal cell carcinoma and in hepatoma have been ascribed to anti-angiogenic actions of this agent through inhibition of the growth factor receptors.[15-17] However, several groups, including ours, have shown *in vitro* that sorafenib kills human leukemia cells at concentrations below the maximum achievable dose (C_{max}) of 15-20 μM, through a mechanism involving down-regulation of the anti-apoptotic BCL-2 family member MCL-1.[18, 19] In these studies sorafenib-mediated MCL-1 down-regulation occurred through a translational rather than a transcriptional or post-translational process that was mediated by endoplasmic reticulum (ER) stress signaling.[20, 21] This suggests that the previously observed anti-tumor effects of sorafenib are mediated by a combination of inhibition of *Raf* family kinases and the ERK1/2 pathway; receptor tyrosine kinases that signal angiogenesis; and the induction of ER stress signaling.

Histone deacetylase inhibitors (HDACI) represent a class of agents that act by blocking histone de-acetylation, thereby modifying chromatin structure and gene transcription. HDACs, along with histone acetyl-transferases, reciprocally regulate the acetylation status of the positively charged NH_2-terminal histone tails of nucleosomes. HDACIs promote histone acetylation and neutralization of positively charged lysine residues on histone tails, allowing chromatin to assume a more open conformation, which favors transcription.[22] However, HDACIs also induce acetylation of other non-histone targets, actions that may have plieotropic biological consequences, including inhibition of HSP90 function, induction of oxidative injury and up-regulation of death receptor expression.[23-25] With respect to combinatorial drug studies with a multi-kinase inhibitor such as sorafenib, HDACIs are of interest in that they also down-regulate multiple oncogenic kinases by interfering with HSP90 function, leading to proteasomal degradation of these proteins. Vorinostat (suberoylanilide hydroxamic acid,

SAHA, Zolinza™) is a hydroxamic acid HDACI that has shown preliminary pre-clinical evidence of activity in hepatoma and other malignancies with a C_{max} of ~9 μM.[26-28] We have recently published that sorafenib and vorinostat to interact to kill in renal, pancreatic and hepatocellular carcinoma cells via activation of the CD95 extrinsic apoptotic pathway, concomitant with drug-induced reduced expression of c-FLIP-s via eIF2α activation.[29] The present studies have extended in greater molecular detail our analyses to include malignant melanoma cells and have mechanistically advanced our understanding to reveal that sorafenib and vorinostat interact by activating acidic sphingomyelinase and the de novo ceramide pathway to promote CD95 activation which regulates both apoptosis and autophagy via PKR like endoplasmic reticulum kinase (PERK).

Materials and Methods

Materials

Sorafenib and Sorafenib tosylate (Bayer) as well as vorinostat (Merck) were provided by the Cancer Treatment and Evaluation Program, National Cancer Institute/NIH (Bethesda, MD). Phospho-/total- (ERK1/2; JNK1/2; p38 MAPK) antibodies, phospho-/total-AKT (T308; S473) and the total and cleaved caspase 3 antibodies were purchased from Cell Signaling Technologies (Worcester, MA). Anti-BID and anti-cathepsin B antibodies were purchased from Cell Signaling Technologies (Worcester, MA). All the secondary antibodies (anti-rabbit-HRP, anti-mouse-HRP, and anti-goat-HRP) were purchased from Santa Cruz Biotechnology (Santa Cruz, CA). Enhanced chemi-luminescence (ECL) and TUNEL kits were purchased from NEN Life Science Products (NEN Life Science Products, Boston, MA) and Boehringer Mannheim (Manheim, Germany), respectively. Trypsin-EDTA, DMEM, RPMI, penicillin-streptomycin were purchased from GIBCOBRL (GIBCOBRL Life Technologies, Grand Island, NY). HEPG2, HEP3B, HuH7 (hepatoma); A498 (renal), CAKI-1, Mia PaCa2, PANC1 (pancreatic), A549, H157 (NSCLC), HMCB, MEL-2, MEL-24, MEL-28, MEL-31 (melanoma) cells were purchased from the ATCC. UOK121LN renal carcinoma cells were kindly provided by Dr. Lineham Marston (National Institutes of Health, Bethesda, MD). BAK -/-, BAK -/-, BID -/- fibroblasts were kindly provided by Dr. S. Korsmeyer (Harvard University, Boston, MA). Immortalized cathepsin B -/- fibroblasts and matched wild type fibroblasts were kindly supplied by Christoph Peters, Thomas Reinheckel (Medizinische Universitaetsklinik Freiburg, Freiburg, Germany) and Paul Saftig (Christian-Albrechts-Universitaet Kiel, Kiel, Germany). Commercially available validated short hairpin RNA molecules to knock down RNA / protein levels were from Qiagen (Valencia, CA): CD95 (SI02654463; SI03118255); FADD (SI00300223; SI03648911); ATG5 (SI02655310); Beclin 1 (SI00055573, SI00055587). We also made use for confirmatory purposes of the short hairpin RNA construct targeting *ATG5* (pLVTHM/Atg5) that was a generous gift from Dr. Yousefi, Department of Pharmacology, University of Bern, Bern Switzerland. The plasmids to express green fluorescent protein (GFP)-tagged human LC3; wild type and dominant negative PERK (Myc-tagged PERKΔC) were kindly provided by Dr. S. Spiegel, VCU and Dr. J.A. Diehl University of Pennsylvania, Philadelphia, PA. Reagents and performance of experimental procedures were described in [20, 21, 29-35].

Methods

Culture and in vitro exposure of cells to drugs—All established cell lines were cultured at 37 °C (5% (v/v CO_2) *in vitro* using RPMI supplemented with 5% (v/v) fetal calf serum and 10% (v/v) Non-essential amino acids. For short term cell killing assays, immunoblotting and AIF/cathepsin release studies, cells were plated at a density of 3×10^3 per cm^2 (~2×10^5 cells per well of a 12 well plate) and 48h after plating treated with various drugs, as indicated. *In vitro* vorinostat and sorafenib treatments were from 100 mM stock solutions of each drug and

the maximal concentration of Vehicle (DMSO) in media was 0.02% (v/v). Cells were not cultured in reduced serum media during any study in this manuscript.

In vitro cell treatments, microscopy, SDS-PAGE and Western blot analysis—For in vitro analyses of short-term cell death effects, cells were treated with Vehicle or vorinostat / sorafenib for the indicated times in the Figure legends. For apoptosis assays where indicated, cells were pre-treated with vehicle (VEH, DMSO), zVAD (50 μM), or Cathepsin B inhibitor ([L-3-*trans*-(Propylcarbamoyl)oxirane-2-carbonyl]-L-isoleucyl-L-proline Methyl ester) (1 μM); cells were isolated at the indicated times, and either subjected to trypan blue cell viability assay by counting in a light microscope or fixed to slides, and stained using a commercially available Diff Quick (Geimsa) assay kit. Alternatively, the Annexin V/propidium iodide assay was carried to determine cell viability out as per the manufacturer's instructions (BD PharMingen) using a Becton Dickinson FACScan flow cytometer (Mansfield, MA). Vorinostat / sorafenib lethality, as judged by annexin-PI, was first evident ~24h after drug exposure (data not shown).

For SDS PAGE and immunoblotting, cells were plated at 5×10^5 cells / cm^2 and treated with drugs at the indicated concentrations and after the indicated time of treatment, lysed in whole-cell lysis buffer (0.5 M Tris-HCl, pH 6.8, 2%SDS, 10% glycerol, 1% β-mercaptoethanol, 0.02% bromophenol blue), and the samples were boiled for 30 min. The boiled samples were loaded onto 10-14% SDS-PAGE and electrophoresis was run overnight. Proteins were electrophoretically transferred onto 0.22 μm nitrocellulose, and immunoblotted with various primary antibodies against different proteins. All immunoblots were visualized by ECL. For presentation, immunoblots were digitally scanned at 600 dpi using Adobe PhotoShop CS2, and their color removed and Figures generated in MicroSoft PowerPoint.

Infection of cells with recombinant adenoviruses—Cells were plated at 3×10^3 per cm^2 in each well of a 12 well, 6 well or 60 mm plate. After plating (24h), cells were infected (hepatoma and pancreatic carcinoma; at a multiplicity of infection of 50; UOK121LN renal carcinoma at a multiplicity of infection of 400) with a control empty vector virus (CMV) and adenoviruses to express CRM A, c-FLIP-s, BCL-XL, XIAP or to express dominant negative AKT / MEK1 / IκB / caspase 9 or activated MEK1 / AKT (Vector Biolabs, Philadelphia, PA). After infection (24h) cells were treated with the indicated concentrations of vorinostat / sorafenib and/or other drugs, and cell survival or changes in expression / phosphorylation determined 0-96h after drug treatment by trypan blue / TUNEL / flow cytometry assays and immunoblotting, respectively.

Transfection of cells with siRNA or with plasmids

For Plasmids: Cells were plated as described above and 24h after plating, transfected. For mouse embryonic fibroblasts (2-5μg) or other cell types (0.5μg) plasmids expressing a specific mRNA (or siRNA) or appropriate vector control plasmid DNA was diluted in 50μl serum-free and antibiotic-free medium (1 portion for each sample). Concurrently, 2μl Lipofectamine 2000 (Invitrogen), was diluted into 50μl of serum-free and antibiotic-free medium (1 portion for each sample). Diluted DNA was added to the diluted Lipofectamine 2000 for each sample and incubated at room temperature for 30 min. This mixture was added to each well / dish of cells containing 200μl serum-free and antibiotic-free medium for a total volume of 300 μl, and the cells were incubated for 4 h at 37 °C. An equal volume of 2x medium was then added to each well. Cells were incubated for 48h, then treated with vorinostat / sorafenib.

Transfection with siRNA: Cells were plated in 60 mm dishes from a fresh culture growing in log phase as described above, and 24h after plating transfected. Prior to transfection, the medium was aspirated and 1 ml serum-free medium was added to each plate. For transfection,

10 nM of the annealed siRNA, the positive sense control doubled stranded siRNA targeting GAPDH or the negative control (a "scrambled" sequence with no significant homology to any known gene sequences from mouse, rat or human cell lines) were used. Ten nM siRNA (scrambled or experimental) was diluted in serum-free media. Four μl Hiperfect (Qiagen) was added to this mixture and the solution was mixed by pipetting up and down several times. This solution was incubated at room temp for 10 min, then added dropwise to each dish. The medium in each dish was swirled gently to mix, then incubated at 37 °C for 2h. One ml of 10% (v/v) serum-containing medium was added to each plate, and cells were incubated at 37 °C for 48h before re-plating (50×10^3 cells each) onto 12-well plates. Cells were allowed to attach overnight, then treated with vorinostat / sorafenib (0-48h). Trypan blue exclusion / TUNEL / flow cytometry assays and SDSPAGE/immunoblotting analyses were performed at the indicated time points.

Isolation of a crude cytosolic fraction—A crude membrane fraction was prepared from treated cells. Briefly, cells were washed twice in ice cold isotonic HEPES buffer (10 mM HEPES pH 7.5, 200 mM mannitol, 70 mM sucrose, 1 μM EGTA, 10 μM protease inhibitor cocktail (Sigma, St. Louis, MO). Cells on ice were scraped into isotonic HEPES buffer and lysed by passing 20 times through a 25 gauge needle. Large membrane pieces, organelles and unlysed cells were removed from the suspension by centrifugation for 5 min at 120 x g. The crude granular fraction and cytosolic fraction was obtained from by centrifugation for 30 min at 10,000 x g, leaving the cytosol as supernatant.

In vivo exposure of carcinoma tumors to drugs—Athymic female NCr-nu/nu mice were obtained from Jackson Laboratories (Bar Harbor, ME). Mice were maintained under pathogen-free conditions in facilities approved by the American Association for Accreditation of Laboratory Animal Care and in accordance with current regulations and standards of the U.S. Department of Agriculture, Washington, DC, the U.S. Department of Health and Human Services, Washington, DC, and the National Institutes of Health, Bethesda, MD. HEP3B cells were cultured and isolated by trypsinization followed by cell number determination using a hemacytometer. Cells were resuspended in phosphate buffered saline and ten million tumor cells per 100 μl PBS were injected into the flank of each mouse, and tumors permitted for 40 days (volume ~150 mm^3). The tumor take rate was ~20%. Vials of vorinostat (stored in a -20° C cold room under vacuum and protected from light; ~30mg / vial) were first dissolved in 30 μl of DMSO, diluted in sterile saline, and heated to boiling for complete dissolution before injection. Mice were administered 25 mg/kg vorinostat by oral gavage based on body mass (0.2 ml total volume per 30 g mouse). Animals received three more administrations of vorinostat, 24h apart for an additional 3 days. Sorafenib was administered 30min prior to the first vorinostat administration each day. Sorafenib tosylate (BAY 54-9085) was dissolved fresh each day. The dosing volume used is 0.3 ml / 30 g body weight. The compound was dissolved in a 50% Cremophor EL / 50% ethanol mixture. The mixture was heated to 60 °C and sonicated for 20 minutes to solubilize. Once the BAY 54-9085 entered solution, the aqueous component was added gradually and with mixing to generate the 1X dosing solution. Animals were administered with BAY 54-9085 for a final concentration of 45 mg/kg. Animals received three more administrations of vorinostat, 24h apart for an additional 3 days. Each animal not receiving a dose of sorafenib or vorinostat at the time of drug treatment was administered diluent alone in a volume equal to the amount given with the drug.

Ex vivo manipulation of tumors—Animals were euthanized by CO_2 and placed in a BL2 cell culture hood on a sterile barrier mat. The bodies of the mice were soaked with 70% (v/v) EtOH and the abdominal skin around the tumor removed using small scissors, forceps and a disposable scalpel. These implements were flame sterilized between removal of the outer and inner layers of skin. A piece of the tumor (~50% by volume) was removed and placed in a 10

cm dish containing 5 ml of RPMI cell culture media, on ice. In parallel portions of the remainder of the tumor were placed in 5 ml of Streck Tissue Fixative (Fisher Scientific, Middletown VA) in a 50 ml conical tube for H&E fixation. The tumor sample that had been placed in RPMI was minced with a sterile disposable scalpel into the smallest possible pieces then placed in a sterile disposable flask. The dish was rinsed with 6.5 ml of RPMI medium which was then added to the flask. A 10x solution of collagenase (Sigma, St. Louis MO; 2.5 ml, 28 U/ml final concentration) and 10x of enzyme mixture containing DNAse (Sigma, St. Louis MO; 308 U/ml final concentration) and pronase (EMD Sciences, San Diego CA; 22,500 U/ml final concentration) in a volume of 1 ml was added to the flask. The flasks were placed into an orbital shaking incubator at 37°C for 1.5 hours at 150 rpm. Following digestion, the solution was passed through a 0.4 μM filter into a 50 ml conical tube. After mixing, a sample was removed for viable and total cell counting using a hemacytometer. Cells were centrifuged at 500 x g for 4 min, the supernatant removed, and fresh RPMI media containing 10% (v/v) fetal calf serum was added to give a final resuspended cell concentration of 1×10^6 cells / ml. Cells were diluted and plated in 10 cm dishes in triplicate at a concentration of 2-6 × 10^3 cells / dish for control, sorafenib and vorinostat treatments and 4-10 × 10^3 / dish for combined sorafenib and vorinostat exposure.

Immunohistochemistry and staining of fixed tumor sections—Post sacrifice, tumors were fixed in OCT compound (Tissue Tek); cryostat sectioned (Leica) as 12 μm sections. Nonspecific binding was blocked with a 2 % (v/v) Rat Sera, 1 % (v/v)Bovine Sera, 0.1% (v/v) Triton X100, 0.05% (v/v) Tween-20 solution then sections were stained for cell signaling pathway markers: Cleaved Caspase 3 (rabbit IgG, 1:100; Cell Signaling); Phospho-AKT 1/2/3 S473 (mouse IgG, 1:100; Santa Cruz); Phospho-ERK1/2 (mouse IgG, 1:100; Santa Cruz); phospho-eIF2 alpha (mouse IgG, 1:100; Santa Cruz); ATG5 (rabbit IgG, 1:100; Cell Signaling). For staining of sectioned tumors, primary antibodies were applied overnight, sections washed with phosphate buffer solution, and secondary antibodies applied for detection (as indicated in the Figure): goat anti-rat Alexa 488/647 (1:500; Invitrogen); goat anti-mouse Alexa 488/647 (1:500; Invitrogen) secondary antibody as per the primary antibody used; or, detected by way of di-aminobenzidine (DAB) substrate Peroxidase Detection Kit (Biogenex), as per the manufacturer's instructions. Sections were then de-hydrated, cleared and mounted with cover-slips using DAPI mounting media (Vectastain). Apoptotic cells with double stranded DNA breaks were detected using the Upstate TUNEL Apototic Detection Kit according to the manufacturer's instructions. Slides were applied to high powered light/confocal microscopes (Zeiss LSM 510 Meta-confocal scanning microscope; Zeiss HBO 100 microscope with Axio Cam MRm camera) at the indicated magnification in the Figure / Figure legend.

Data analysis—Comparison of the effects of various treatments was performed using ANOVA and the Student's t test. Differences with a *p*-value of < 0.05 were considered statistically significant. Experiments shown are the means of multiple individual points (± SEM). Median dose effect isobologram analyses to determine synergism of drug interaction were performed according to the Methods of T.-C. Chou and P. Talalay using the Calcusyn program for Windows (BIOSOFT, Cambridge, UK). Cells are treated with agents at a fixed concentration dose. A combination index (CI) value of less than 1.00 indicates synergy of interaction between the drugs; a value of 1.00 indicates additivity; a value of > 1.00 equates to antagonism of action between the agents.

Results

Treatment of transformed fibroblasts that had altered expression / activity within various survival regulatory pathways with vorinostat and sorafenib demonstrated that loss of BAX and BAK expression and loss of BID expression abolished the toxic interaction between vorinostat

and sorafenib (Figure 1a). Inhibition of PERK-eIF2α stress signaling modestly enhanced the lethality of low doses of sorafenib as a single agent, in agreement with previous observations in leukemic cells however, loss of PERK-eIF2α endoplasmic reticulum (ER) stress signaling abolished the toxic interaction between vorinostat and sorafenib (Figure 1a).[21,29] Low concentrations of vorinostat and sorafenib rapidly suppressed the expression of c-FLIP-s, but not of c-FLIP-l, in renal and hepatocellular carcinoma cells (Figure 1b, section (i), data not shown). Inhibition of c-FLIP-s expression was dependent upon eIF2α as judged by expression of dominant negative eIF2α S51A blocking the reduction of c-FLIP-s levels (Figure 1b, section (ii)). Low concentrations of vorinostat and sorafenib promoted release of cytochrome c into the cytosol that was blocked by over-expression of c-FLIP-s (Figure 1c, section (i)). Vorinostat and sorafenib lethality was abolished by over-expression of exogenous c-FLIP-s or eIF2α S51A (Figure 1c, section (ii)). [21,29]

Malignant melanoma was one of the initial malignancies chosen as a target for the exploration of sorafenib efficacy based on the concept that the primary target of sorafenib in tumor cells was the *Raf* family of protein kinases, and in particular, mutated active forms of B-Raf.[2, 12] We next investigated whether sorafenib and vorinostat interacted to kill malignant melanoma cells, and if so, by what mechanism this occurred. Sorafenib and vorinostat interacted in a greater than additive fashion to kill malignant melanoma cells (Figure 1d). Treatment of MEL-2 cells with sorafenib and vorinostat caused rapid activation of CD95 and DISC formation (Figure 1e, upper blotting panels). Prior studies have noted that treatment with the individual agents sorafenib or vorinostat at these low concentrations used did not promote CD95 surface localization or DISC formation. [29] Knock down of CD95 expression or over-expression of c-FLIP-s abolished sorafenib and vorinostat toxicity (Figures 1d and 1e, lower graphical panels). Sorafenib and vorinostat synergized to kill MEL-2 and MEL-31 melanoma cells, and A549 and H157 NSCLC cells, in long term colony formation assays with combination index (CI) values of less than 1.00; effects that were abolished by over-expression of the caspase 8 inhibitor c-FLIP-s (Table 1, data not shown).

Based on data showing that inhibition of PERK and eIF2α function suppressed sorafenib and vorinostat lethality we examined whether these agents modulated the expression of other markers of ER stress and autophagy signaling. Treatment of cells in vitro with low doses of sorafenib and vorinostat, but not the individual agents alone at these low doses, rapidly increased phosphorylation of PERK and eIF2α, increased processing of LC3, and increased expression of ATG5 (Figure 2a). Similar data were also obtained in melanoma cells (not shown). The ATG12-ATG5 and the ATG8 (LC3)-PE conjugation systems are interdependent and a disruption in one system has a direct negative effect on the autophagic process. In established ~150-200 mm^3 flank HEP3B tumors, treatment with sorafenib and vorinostat, but not exposure to the individual drugs, enhanced phosphorylation of eIF2α (Figure 2b). In ~150-200 mm^3 flank HEP3B tumors, treatment with sorafenib and with sorafenib and vorinostat, but not with vorinostat alone, enhanced ATG5 expression (Figure 2b). The ex vivo long-term colony formation of tumor cells treated with vorinostat and sorafenib was reduced in a greater than additive fashion (data not shown).[29] Of particular note, sorafenib and vorinostat lethality in vivo (increased caspase 3 cleavage; TUNEL+) correlated with increased eIF2α phosphorylation, increased ATG5 expression, decreased c-FLIP-s expression, decreased AKT phosphorylation but not with dephosphorylation ERK1/2 (Figure 2b), further suggesting that a simplistic correlation between sorafenib toxicity and ERK1/2 pathway inactivation cannot be implied from our data.

As LC3 was being rapidly processed and ATG5 expression enhanced by combined sorafenib and vorinostat treatment in vitro, but not by exposure to the individual drugs, we explored whether autophagy was being induced in sorafenib and vorinostat treated cells. Vacuole localization of the protein LC3 is one recognized marker for the induction of autophagy, and

transfection of HEPG2 cells with a construct to express a green fluorescent protein (GFP) tagged LC3 protein demonstrated that combined sorafenib and vorinostat treatment rapidly induced and sustained vacuolization of GFP tagged LC3 within 6h-24h (Figure 2c).

Previous studies have shown that sorafenib lethality and ER stress signaling is not related to its inhibitory actions on *Raf* family kinases.[21] We next determined whether inhibition of "off target" protein kinases for sorafenib, the class III family of receptor tyrosine kinases, were involved in regulating the LC3-GFP vesicularization effects caused after exposure to high individual concentrations of sorafenib. Knock down of PDGFβ receptor expression enhanced basal levels of GFP-LC3 vesicularization in HEPG2 cells and abolished high dose sorafenib-induced GFP-LC3 vesicularization (Figure 2d). Knock down of FLT3 expression suppressed sorafenib-induced GFP-LC3 vesicularization. Identical data to those in HEPG2 cells were obtained in UOK121LN renal carcinoma cells (data not shown).

In prior studies we had noted that inhibition of cathepsin protease function suppressed sorafenib and vorinostat toxicity.[29] We next attempted to place the activation of cathepsin B within the context of sorafenib and vorinostat -induced vacuolization. Loss of cathepsin B expression did not, statistically, alter sorafenib and vorinostat -LC3-GFP vacuolization but abolished the ability of sorafenib and vorinostat treatment to cause a later acidic endosome acidification, as judged by reduced lysotracker red staining in the cathepsin B -/- cells compared to WT cells treated with the drug combination (Figure 2e, top and bottom sections). Furthermore, GFP-LC3 punctate staining and lysotracker red staining did not co-localize in drug treated wild type cells (Figure 2e, middle section). Thus, in a similar manner to MDA-7/IL-24 and OSU-03012, the apparent secondary lysotracker red staining / acidic endosome vacuolization after drug -induced LC3 vesicle formation was a secondary cathepsin B dependent process.[31, 32]

We next investigated whether there were any mechanistic links between vorinostat and sorafenib lethality, the activation of CD95, ER stress signaling, and the induction of autophagy. Sorafenib and vorinostat activated CD95 whose activation / surface localization / surface clustering was not altered by expression of dominant negative PERK or by knock down of ATG5 expression (Figure 3a). Sorafenib and vorinostat treatment caused formation of a classic "DISC" with CD95 immunoprecipitates after drug exposure comprising of pro-caspase 8 and FADD, however, expression of dominant negative PERK abolished the drug-induced formation of the DISC (Figure 3b, upper section). Expression of dominant negative PERK also abolished the induction of ATG5 expression after drug exposure (Figure 3b, lower section). Expression of dominant negative PERK or knock down of ATG5 expression abolished the drug-induced induction of autophagy (Figure 3c). In general agreement with data in Figure 1a, and with data in Figure 3a, expression of dominant negative PERK significantly reduced the lethality of vorinostat and sorafenib (Figure 3d). This correlated with reduced cleavage of pro-caspase 8. However, knock down of ATG5 enhanced the lethality of vorinostat and sorafenib treatment. This correlated with enhanced cleavage of pro-caspase 8 and with enhanced levels of caspase 8 in the DISC.

Previously we noted that treatment of cells with vorinostat and sorafenib rapidly activated both CD95 and PERK (Figures 1f and 2a, data not shown).[29] Based on the apparent signaling association between CD95 and PERK observed in Figure 3, we next determined whether the activation of PERK was dependent upon activation / surface localization of CD95. Knock down of CD95 or of FADD expression abolished the drug-induced phosphorylation of PERK and eIF2α and increased expression of ATG5 (Figure 4a). If PERK activation was dependent on CD95 expression; and enhanced ATG5 expression and the induction of autophagic vesicle formation were also dependent on PERK signaling after drug exposure, we reasoned that the induction of autophagy should be dependent on the activation of CD95 and FADD. In agreement with this hypothesis, knock down of CD95 and to a modest lesser extent FADD,

expression suppressed the induction of autophagy in vorinostat and sorafenib treated cells (Figure 4b).

The "classic" components of a DISC complex upon FAS ligand-stimulated activation of CD95 include FADD, pro-caspase 8 and FLIP proteins.[36-38] More recently, in yeast two hybrid studies, ATG5 has been noted to associate with FADD.[39] We discovered in CD95 immunoprecipitates, after vorinostat and sorafenib exposure, that pro-caspase 8, ATG5 and Grp78/BiP co-immunoprecipitated in a FADD and PERK -dependent fashion (Figure 4c, immunoblotting panel to the left). As CD95 activated PERK, we next determined whether PERK associated with CD95 after drug exposure. We transfected cells with two MYC-tagged forms of PERK; wild type PERK and a dominant negative kinase inactive form of PERK, and immunoblotted CD95 immunoprecipitates for the tagged PERK protein after vorinostat and sorafenib treatment.[21] Vorinostat and sorafenib exposure promoted a stable association between wild type PERK and CD95 6h after drug exposure, however, there was no stable association as judged following immunoprecipitation induced between dominant negative PERK and CD95 after drug exposure (Figure 4c, immunoblotting panel to the right).

The present, as well as prior, analyses have shown that over-expression of c-FLIP-s prevented cell killing by vorinostat and sorafenib exposure in short term and long term cell viability assays.[29] Based on the fact that loss of ATG5 promoted caspase 8 levels within the DISC, that c-FLIP-s inhibits caspase 8, and is part of the "classical" DISC complex; we investigated whether over-expression of c-FLIP-s simply blocks death signaling by inhibiting caspase 8 or impacted *positively* to promote survival via "shunting" CD95 signaling towards the induction of autophagy.[29] Over-expression of c-FLIP-s promoted autophagic vesicle formation after vorinostat and sorafenib exposure (Figure 4d; see also Figure 1f and DISC formation data).[29]

Prior studies in this manuscript in melanoma cells and those in hepatoma and renal carcinoma cells demonstrated that vorinostat and sorafenib exposure activate CD95; in HEPG2 cells, the activation of CD95 was ligand independent as receptor activation occurred without increases in CD95 protein levels or cleavage of FAS-L.[29] One mechanism by which ligand-independent activation of CD95 has been proposed to occur is via activation of acidic sphingomyelinase (ASMase) and the generation of the lipid second messenger ceramide.[34, 37, 38] Increased ceramide levels promote the clustering of CD95 molecules into lipid rafts, thereby facilitating receptor trimerization and activation.[40] Treatment of HEPG2 or primary mouse hepatocytes with vorinostat and sorafenib increase surface localization of CD95 in these cells (Figure 5a). Knock down of ASMase expression in HEPG2 cells abolished the vorinostat and sorafenib -stimulated increase surface localization of CD95. Genetic deletion of ASMase expression in primary mouse hepatocytes abolished the vorinostat and sorafenib -stimulated increase surface localization of CD95 (Figure 5a).

Based on the data in Figure 5a, we next measured ceramide levels in sorafenib and vorinostat treated cells 3h after drug exposure, at the earliest time we were observing any CD95 surface localization / activation (data not shown). This time point was chosen to minimize any potential involvement of ASMase activation caused by CD95 activation itself i.e. in a self-stimulatory loop. Treatment of HEPG2 cells with sorafenib and vorinostat modestly increased C14 and C16 ceramide levels that were abolished by knock down of ASMase (Table 2, upper section); other induced forms of ceramide were not affected by knock down of ASMase.

As knock down of acidic sphingomyelinase did not profoundly reduce the amount of ceramide being generated following drug exposure we determined whether the increase in ceramide species levels and activation of CD95 also resulted from enhanced *de novo* biosynthesis or salvage pathway and recycling of sphingosine effects; cells were pretreated with myriocin, a

specific inhibitor of serine palmitoyltransferase, the rate-limiting step in *de novo* synthesis or with fumonisin B1, an inhibitor of dihydroceramide/ceramide synthases that acylate sphingoid bases. Treatment of cells with either fumonisin B1 or myriocin abolished drug-induced surface localization, i.e. activation, of CD95 (Figure 5b). Treatment of cells with fumonisin B1 significantly reduced the drug-induced increase in several di-hydro ceramide species (Table 2, lower section). In the case of dihydro-ceramide species with chain lengths of C12, C22-1 and C26 the drug-induced increase in lipid levels was statistically abolished by Fumonisin B1 treatment. These findings argue that the *de novo* ceramide synthesis pathway is activated by vorinostat and sorafenib treatment and that signaling by both the *de novo* and acidic sphingomyelinase ceramide generation pathways are required to permit CD95 to become membrane localized and signal cell death and autophagy after drug exposure. In agreement with the roles of the ASMase and de novo synthesis pathways in regulating CD95 function, inhibition of both the ASMase pathway and de novo ceramide generation pathway significantly reduced sorafenib and vorinostat lethality (Figure 5c).

Discussion

Previous studies from our laboratories have shown that sorafenib and vorinostat interact in vitro and in vivo in a greater than additive fashion to kill transformed cells. In hepatoma and in renal and pancreatic carcinoma cells sorafenib and vorinostat -induced cell killing was mechanistically dependent on activation of CD95 and inhibition of c-FLIP-s expression.[29] The present studies attempted to determine in much greater detail the molecular mechanisms by which sorafenib and vorinostat activated CD95 and the cell survival regulatory pathways downstream of CD95, but proximal to the receptor, that control drug-induced toxicity.

The results of the present study indicate that low concentrations of sorafenib and vorinostat interact in a synergistic manner to also kill malignant melanoma cells in vitro. In vitro, the enhanced lethality of the regimen toward melanoma cells was also blocked by inhibition of CD95 function and abolished by over-expression of c-FLIP-s. Of particular note, neither as a single agent nor when combined with vorinostat, did we observe sorafenib lethality correlating with expression of mutated active B-Raf in melanoma cells. Our findings provide further confirmation in a cell type that is embryologically distinct from hepatoma, renal and pancreatic carcinoma cells that a central mechanism of low dose sorafenib and vorinostat lethality involves primary activation of the CD95 extrinsic apoptosis pathway, with diminished c-FLIP-s levels, which in turn facilitate secondary activation of the downstream intrinsic apoptosis pathway (Figure 5d).

Previously we noted that the reduction in c-FLIP-s levels after sorafenib and vorinostat treatment was eIF2α dependent.[29] In the present study we discovered that eIF2α phosphorylation after drug exposure was PERK dependent, correlating with PERK phosphorylation, arguing that sorafenib and vorinostat caused an apparent form of ER stress. Prior studies from this group have shown that sorafenib as a single agent in the very high dose ~10-15 μM range, which are still within pharmacologically achievable concentrations induced cell death in human leukemic cells by promoting ER stress and diminishing expression of MCL-1 rather than by inhibiting either *Raf* family kinases or putatively by blocking receptor tyrosine kinases.[14-16, 20, 21] Our present studies demonstrated that higher concentrations of sorafenib in the ~6 μM range did cause autophagy, in part, by blocking PDGFRβ and FLT3 signaling. The interactions between much higher concentrations of sorafenib and the extrinsic pathway agonist TRAIL in malignant hematopoietic cells have been related to inhibition of c-FLIP translation.[41] Others, also using much higher concentrations of sorafenib have observed c-FLIP and MCL-1 expression suppression by this agent, which is likely due to suppression of transcription and translation.[42] Thus suppression of protein translation by sorafenib (*cf* the present data showing increased PERK and eIF2α phosphorylation).[18, 19] events which induce

c-FLIP-s down-regulation as well as inhibition of MCL-1 levels, may represent a common mechanism by which sorafenib lethality is enhanced by vorinostat in carcinoma cells.

Previously we have shown that bile acids can promote ligand independent, ASMase and ceramide -dependent, activation of CD95 in primary hepatocytes.[11, 34, 35] Recent studies have confirmed these findings. [51] The generation of ceramide has been shown by many groups to promote ligand independent activation of several growth factor receptors via the localization / clustering of these receptors and other signal facilitating proteins into lipid rich domains.[43, 44] Our analyses in HEPG2 cells demonstrated that loss of ASMase function reduced formation of C14 and C16 ceramide species whereas inhibition of the de novo synthesis pathway modestly suppressed generation of multiple dihydro-ceramide species. The six known ceramide synthase genes (LASS) are localized in the ER and different LASS proteins have been noted to generate different chain length ceramide forms.[50] Based on our data, with Fumonisin B1-inhibiting the drug-induced increases in C12 / C14 / C16 and C20 / C24 / C26 dihydro-ceramide levels, it is possible that vorinostat and sorafenib may be modulating the activities of LASS6 and LASS5, respectively.[50] Whether any of the different forms of ceramide and LASS genes truly preferentially promote CD95 surface localization, membrane clustering or association with other membrane proteins will need to be addressed in future studies.

Activation of CD95 has been shown to promote the formation of several associated complexes of proteins with the receptor on the intracellular side of the plasma membrane. The most widely recognized of these complexes is the “DISC” in which the FAS associated death domain (FADD) protein associates with CD95 and with pro-caspase 8 (and pro-caspase 10), leading to the auto-catalytic cleavage of pro-caspases.[45] The actions of c-FLIP-s and c-FLIP-l can prevent caspase activation, although c-FLIP-l has in some studies been argued to facilitate caspase 8 activation.[45, 46] The protein kinase RIP also contains a death domain and can be found in the DISC; RIP has been proposed to be acted upon by activated caspase 8 to signal cell death or cell survival process in a cell type dependent fashion.[46] Our prior studies demonstrated that vorinostat and sorafenib treatment did not differentially modulate JNK1/2 or p38 MAPK signaling, but did argue that NFκB was involved in promoting cell death, suggesting that RIP may play a role in drug toxicity after combined exposure. Pyo et al. have suggested that ATG5 can interact with FADD to modulate survival after interferon γ exposure and it is known that the RNA-activated kinase, PKR, can induce cell killing that is often mediated via a FADD-caspase 8 pathway.[39, 47] Our present findings demonstrated that PERK, ATG5 and Grp78/BiP all associated with sorafenib and vorinostat -activated CD95 and that the interaction occurred via association with FADD. Two of these proteins represent novel stress-/drug-induced DISC components.

We found that vorinostat and sorafenib -induced activation of CD95 generates both survival and cytotoxic signals, with the relative outcome of signaling being pro-apoptotic provided that no *impediment* is placed upon the migration of the toxic cell signal away from the death receptor. In the drug treatment system used in this manuscript, vorinostat and sorafenib, autophagy represents a survival signal whereas in other systems recently examined by our laboratory, autophagic signaling was noted to play an active role in promoting cell death.[31, 32] In these other systems, using OSU-03012 or GST-MDA-7, the induction of autophagy followed by cell killing was *independent* of CD95 / caspase 8 / c-FLIP-s, function suggesting that CD95-dependent and -independent stimulated forms of autophagy coexist whilst still utilizing proteins such as ATG5 and Beclin1 to promote vesicle formation.

One key difference comparing the induction of autophagy between the drug-induced forms of autophagy discussed in the last paragraph is the apparent involvement of the protein c-FLIP-s; with vorinostat and sorafenib -induced killing we noted previously that sustained c-FLIP-s

expression resulted in blockade of BID cleavage, and in the present studies that sustained c-FLIP-s expression reduced the amount of pro-caspase 8 co-immunoprecipitating with CD95 and caused the levels of autophagy to increase.[29] The present findings suggest that in the presence of high levels of c-FLIP-s activation of a death receptor may not simply be negated by over-expression of c-FLIP-s; activation of a death receptor may be actively subverted by c-FLIP-s towards an autophagic survival signal that could have potential to improve tumor cell viability in response to other stresses. Furthermore, that c-FLIP-s over-expression suppressed sorafenib and vorinostat cell killing but simultaneously increased sorafenib and vorinostat autophagy that may be a mechanism by which sorafenib and vorinostat activity is limited in vivo. Inhibition of the autophagic pathway may thus be one mechanism by which we could augment sorafenib and vorinostat activity in vivo. The "DISC" complex containing caspase 8 has been known for many years and in protein kinase signal transduction in both yeast and mammalian biology, the concept of a multi-protein "*signalosome*" containing many protein kinases docked to a transducing protein such as kinase-suppressor-of-ras (KSR) has also been proposed and established for a decade.[48, 49] Recently we have published near identical data to that in this manuscript in primary hepatocytes over-expressing the cyclin dependent kinase inhibitors p21 or p27, and treated with bile acids and a MEK1/2 inhibitor. [51] Over-expression of p21 or p27 promoted ASMase-, CD95- and PERK-dependent apoptosis and autophagy in these cells; autophagy was protective. Hence the discovery that multiple proteins which regulate endoplasmic reticulum stress signaling and autophagy also form a signaling complex with an activated death receptor and its associated death domain protein, and that this occurs in multiple cell systems with multiple stress stimuli, expands this concept.

In conclusion, the results of the present study indicate that sorafenib and vorinostat interact in a highly synergistic manner to kill a wide variety of tumor cells in vitro via activation of CD95. Ongoing in vitro, animal and multiple phase I patient studies will continue to define the importance of sorafenib and vorinostat as a therapeutic in epithelial cell malignancies.

Acknowledgements

This work was funded; to P.D. from PHS grants (R01-DK52825, P01-CA104177, R01-CA108520); to S.G. from PHS grants (R01-CA63753; R01-CA77141) and a Leukemia Society of America grant 6405-97. The measurement of ceramide was performed by the MUSC Lipidomics core funded by grant C06-RR018823. These studies were also funded in part by The Jimmy V Foundation. A portion of Dr. Yacoub's funding is from the Department of Radiation Oncology, Virginia Commonwealth University and PD is the holder of the Universal Inc. Professorship in Signal Transduction Research.

Abbreviations

Vor., Vorinostat
Sor., Sorafenib
ERK, extracellular regulated kinase
MEK, mitogen activated extracellular regulated kinase
EGF, epidermal growth factor
PARP, poly ADP ribosyl polymerase
PI3K, phosphatidyl inositol 3 kinase
-/-, null / gene deleted
ERK, extracellular regulated kinase
MAPK, mitogen activated protein kinase
MEK, mitogen activated extracellular regulated kinase
R, receptor
JNK, c-Jun NH_2-terminal kinase
dn, dominant negative
P, phospho-

ca, constitutively active
WT, wild type

References

1. Parkin DM, Bray F, Ferlay J, Pisani P. Global cancer statistics, 2002. CA Cancer J Clin 2005;55:74–108. [PubMed: 15761078]
2. Tsao H. Management of Cutaneous Melanoma. N Engl J Med 2004;351:998–1012. [PubMed: 15342808]
3. Dent, P. MAP kinase pathways in the control of hepatocyte growth, metabolism and survival. Dufour, JF.; Clavien, P-A., editors. Signaling Pathways in Liver Diseases, Springer Press; 2005. p. 223-238.Chapter 19
4. Dent P, Yacoub A, Fisher PB, Hagan MP, Grant S. MAPK pathways in radiation responses. Oncogene 2003;22:5885–96. [PubMed: 12947395]
5. Valerie K, Yacoub A, Hagan MP, et al. Radiation-induced cell signaling: inside-out and outside-in. Mol Cancer Ther 2007;6:789–801. [PubMed: 17363476]
6. Grant S, Dent P. Kinase inhibitors and cytotoxic drug resistance. Clin Cancer Res 2004;10:2205–7. [PubMed: 15073093]
7. Allan LA, Morrice N, Brady S, Magee G, Pathak S, Clarke PR. Inhibition of caspase-9 through phosphorylation at Thr 125 by ERK MAPK. Nat Cell Biol 2003;5:647–54. [PubMed: 12792650]
8. Mori M, Uchida M, Watanabe T, et al. Activation of extracellular signal-regulated kinases ERK1 and ERK2 induces Bcl-xL up-regulation via inhibition of caspase activities in erythropoietin signaling. J Cell Physiol 2003;195:290–7. [PubMed: 12652655]
9. Ley R, Balmanno K, Hadfield K, Weston C, Cook SJ. Activation of the ERK1/2 signaling pathway promotes phosphorylation and proteasome-dependent degradation of the BH3-only protein, Bim. J Biol Chem 2003;278:18811–6. [PubMed: 12646560]
10. Wang YF, Jiang CC, Kiejda KA, Gillespie S, Zhang XD, Hersey P. Apoptosis induction in human melanoma cells by inhibition of MEK is caspase-independent and mediated by the Bcl-2 family members PUMA, Bim, and Mcl-1. Clin Cancer Res 2007;13:4934–42. [PubMed: 17652623]
11. Qiao L, Han SI, Fang Y, et al. Bile acid regulation of C/EBPbeta, CREB, and c-Jun function, via the extracellular signal-regulated kinase and c-Jun NH2-terminal kinase pathways, modulates the apoptotic response of hepatocytes. Mol Cell Biol 2003;23:3052–66. [PubMed: 12697808]
12. Li N, Batt D, Warmuth M. B-Raf kinase inhibitors for cancer treatment. Curr Opin Investig Drugs 2007;8:452–6.
13. Davies BR, Logie A, McKay JS, et al. AZD6244 (ARRY-142886), a potent inhibitor of mitogen-activated protein kinase/extracellular signal-regulated kinase kinase 1/2 kinases: mechanism of action in vivo, pharmacokinetic/pharmacodynamic relationship, and potential for combination in preclinical models. Mol Cancer Ther 2007;6:2209–19. [PubMed: 17699718]
14. Flaherty KT. Sorafenib: delivering a targeted drug to the right targets. Expert Rev Anticancer Ther 2007;7:617–26. [PubMed: 17492926]
15. Rini BI. Sorafenib. Expert Opin Pharmacother 2006;7:453–61. [PubMed: 16503817]
16. Strumberg D. Preclinical and clinical development of the oral multikinase inhibitor sorafenib in cancer treatment. Drugs Today (Barc) 2005;41:773–84. [PubMed: 16474853]
17. Gollob JA. Sorafenib: scientific rationales for single-agent and combination therapy in clear-cell renal cell carcinoma. Clin Genitourin Cancer 2005;4:167–74. [PubMed: 16425993]
18. Rahmani M, Davis EM, Bauer C, Dent P, Grant S. Apoptosis induced by the kinase inhibitor BAY 43-9006 in human leukemia cells involves down-regulation of Mcl-1 through inhibition of translation. J Biol Chem 2005;280:35217–27. [PubMed: 16109713]
19. Rahmani M, Nguyen TK, Dent P, Grant S. The multikinase inhibitor sorafenib induces apoptosis in highly imatinib mesylate-resistant bcr/abl+ human leukemia cells in association with signal transducer and activator of transcription 5 inhibition and myeloid cell leukemia-1 down-regulation. Mol Pharmacol 2007;72:788–95. [PubMed: 17595328]

20. Dasmahapatra G, Yerram N, Dai Y, Dent P, Grant S. Synergistic interactions between vorinostat and sorafenib in chronic myelogenous leukemia cells involve Mcl-1 and p21CIP1 down-regulation. Clin Cancer Res 2007;13:4280–90. [PubMed: 17634558]
21. Rahmani M, Davis EM, Crabtree TR, et al. The kinase inhibitor sorafenib induces cell death through a process involving induction of endoplasmic reticulum stress. Mol Cell Biol 2007;27:5499–513. [PubMed: 17548474]
22. Gregory PD, Wagner K, Horz W. Histone acetylation and chromatin remodeling. Exp. Cell Res 2001;265:195–202. [PubMed: 11302684]
23. Marks PA, Miller T, Richon VM. Histone deacetylases. Curr Opin Pharmacol 2003;3:344–351. [PubMed: 12901942]
24. Bali P, Pranpat M, Swaby R, et al. Activity of suberoylanilide hydroxamic Acid against human breast cancer cells with amplification of her-2. Clin Cancer Res 2005;11:6382–9. [PubMed: 16144943]
25. Kwon SH, Ahn SH, Kim YK, et al. Apicidin, a histone deacetylase inhibitor, induces apoptosis and Fas/Fas ligand expression in human acute promyelocytic leukemia cells. J Biol Chem 2002;277:2073–80. [PubMed: 11698395]
26. Pang RW, Poon RT. From molecular biology to targeted therapies for hepatocellular carcinoma: the future is now. Oncology 2007;72(Suppl 1):30–44. [PubMed: 18087180]
27. Venturelli S, Armeanu S, Pathil A, et al. Epigenetic combination therapy as a tumor-selective treatment approach for hepatocellular carcinoma. Cancer 2007;109:2132–41. [PubMed: 17407132]
28. Wise LD, Turner KJ, Kerr JS. Assessment of developmental toxicity of vorinostat, a histone deacetylase inhibitor, in Sprague-Dawley rats and Dutch Belted rabbits. Birth Defects Res B Dev Reprod Toxicol 2007;80:57–68. [PubMed: 17294457]
29. Zhang G, Park M, Mitchell C, et al. Vorinostat and sorafenib synergistically kill tumor cells via FLIP suppression and CD95 activation. Clin Cancer Res. 2008IN PRESS
30. Mitchell C, Park MA, Zhang G, Yacoub A, Curiel DT, Fisher PB, Roberts JD, Grant S, Dent P. Extrinsic pathway- and cathepsin-dependent induction of mitochondrial dysfunction are essential for synergistic flavopiridol and vorinostat lethality in breast cancer cells. Mol Cancer Ther 2007;6:3101–12. [PubMed: 18065490]
31. Park MA, Yacoub A, Rahmani M, et al. OSU-03012 stimulates PERK-dependent increases in HSP70 expression, attenuating its lethal actions in transformed cells. Mol Pharm. 2008In Press
32. Yacoub A, Park MA, Gupta P, et al. Caspase-, cathepsin- and PERK-dependent regulation of MDA-7/IL-24-induced cell killing in primary human glioma cells. Mol Cancer Ther. 2008In Press
33. Mitchell C, Park MA, Zhang G, Han SI, Harada H, Franklin RA, Yacoub A, Li PL, Hylemon PB, Grant S, Dent P. 17-Allylamino-17-demethoxygeldanamycin enhances the lethality of deoxycholic acid in primary rodent hepatocytes and established cell lines. Mol Cancer Ther 2007;6:618–32. [PubMed: 17308059]
34. Gupta S, Natarajan R, Payne SG, Studer EJ, Spiegel S, Dent P, Hylemon PB. Deoxycholic acid activates the c-Jun N-terminal kinase pathway via FAS receptor activation in primary hepatocytes. Role of acidic sphingomyelinase-mediated ceramide generation in FAS receptor activation. J Biol Chem 2001;279:5821–8. [PubMed: 14660582]
35. Qiao L, Studer E, Leach K, et al. Deoxycholic acid (DCA) causes ligand-independent activation of epidermal growth factor receptor (EGFR) and FAS receptor in primary hepatocytes: inhibition of EGFR/mitogen-activated protein kinase-signaling module enhances DCA-induced apoptosis. Mol Biol Cell 2001;12:2629–45. [PubMed: 11553704]
36. Gillenwater AM, Zhong M, Lotan R. Histone deacetylase inhibitor suberoylanilide hydroxamic acid induces apoptosis through both mitochondrial and Fas (Cd95) signaling in head and neck squamous carcinoma cells. Mol Cancer Ther 2007;6:2967–75. [PubMed: 18025281]
37. Park SM, Schickel R, Peter ME. Nonapoptotic functions of FADD-binding death receptors and their signaling molecules. Curr Opin Cell Biol 2005;17:610–6. [PubMed: 16226446]
38. Barnhart BC, Alappat EC, Peter ME. The CD95 type I/type II model. Semin Immunol 2003;15:185–93. [PubMed: 14563117]
39. Pyo JO, Jang MH, Kwon YK, et al. Essential roles of Atg5 and FADD in autophagic cell death: dissection of autophagic cell death into vacuole formation and cell death. J Biol Chem 2005;280:20722–9. [PubMed: 15778222]

40. Peták I, Houghton JA. Shared pathways: death receptors and cytotoxic drugs in cancer therapy. Pathol Oncol Res 2001;7:95–106. [PubMed: 11458271]
41. Rosato RR, Almenara JA, Coe S, Grant S. The multikinase inhibitor sorafenib potentiates TRAIL lethality in human leukemia cells in association with Mcl-1 and cFLIPL down-regulation. Cancer Res 2007;67:9490–500. [PubMed: 17909059]
42. Ricci MS, Kim SH, Ogi K, et al. Reduction of TRAIL-induced Mcl-1 and cIAP2 by c-Myc or sorafenib sensitizes resistant human cancer cells to TRAIL-induced death. Cancer Cell 2007;12:66–80. [PubMed: 17613437]
43. Reinehr R, Häussinger D. Hyperosmotic activation of the CD95 system. Methods Enzymol 2007;428:145–60. [PubMed: 17875416]
44. Bollinger CR, Teichgräber V, Gulbins E. Ceramide-enriched membrane domains. Biochim Biophys Acta 2005;1746:284–94. [PubMed: 16226325]
45. Kataoka T. The caspase-8 modulator c-FLIP. Crit Rev Immunol 2005;25:31–58. [PubMed: 15833082]
46. Walsh CM, Luhrs KA, Arechiga AF. The “fuzzy logic” of the death-inducing signaling complex in lymphocytes. J Clin Immunol 2003;23:333–53. [PubMed: 14601642]
47. García MA, Meurs EF, Esteban M. The dsRNA protein kinase PKR: virus and cell control. Biochimie 2007;89:799–811. [PubMed: 17451862]
48. Kolch W. Coordinating ERK/MAPK signalling through scaffolds and inhibitors. Nat Rev Mol Cell Biol 2005;6:827–37. [PubMed: 16227978]
49. Bielawski J, Szulc ZM, Hannun YA, Bielawska A. Simultanous Quantitative Analysis of Bioactive Sphingolipids by High Performance Liquid Chromatography-Tandem Mass Spectrometry. Methods 2006;39:82–91. [PubMed: 16828308]
50. Zhang G, Park MA, Mitchell C, Walker T, Hamed H, Studer E, Graf M, Gupta S, Hylemon PB, Fisher PB, Grant S, Dent P. Multiple cyclin kinase inhibitors promote bile acid -induced apoptosis and autophagy in primary hepatocytes via p53 - CD95 -dependent signaling. J Biol Chem. 2008IN PRESS
51. Pewzner-Jung Y, Ben-Dor S, Futerman AH. When do Lasses (longevity assurance genes) become CerS (ceramide synthases)?: Insights into the regulation of ceramide synthesis. J Biol Chem 2006;281:25001–5. [PubMed: 16793762]

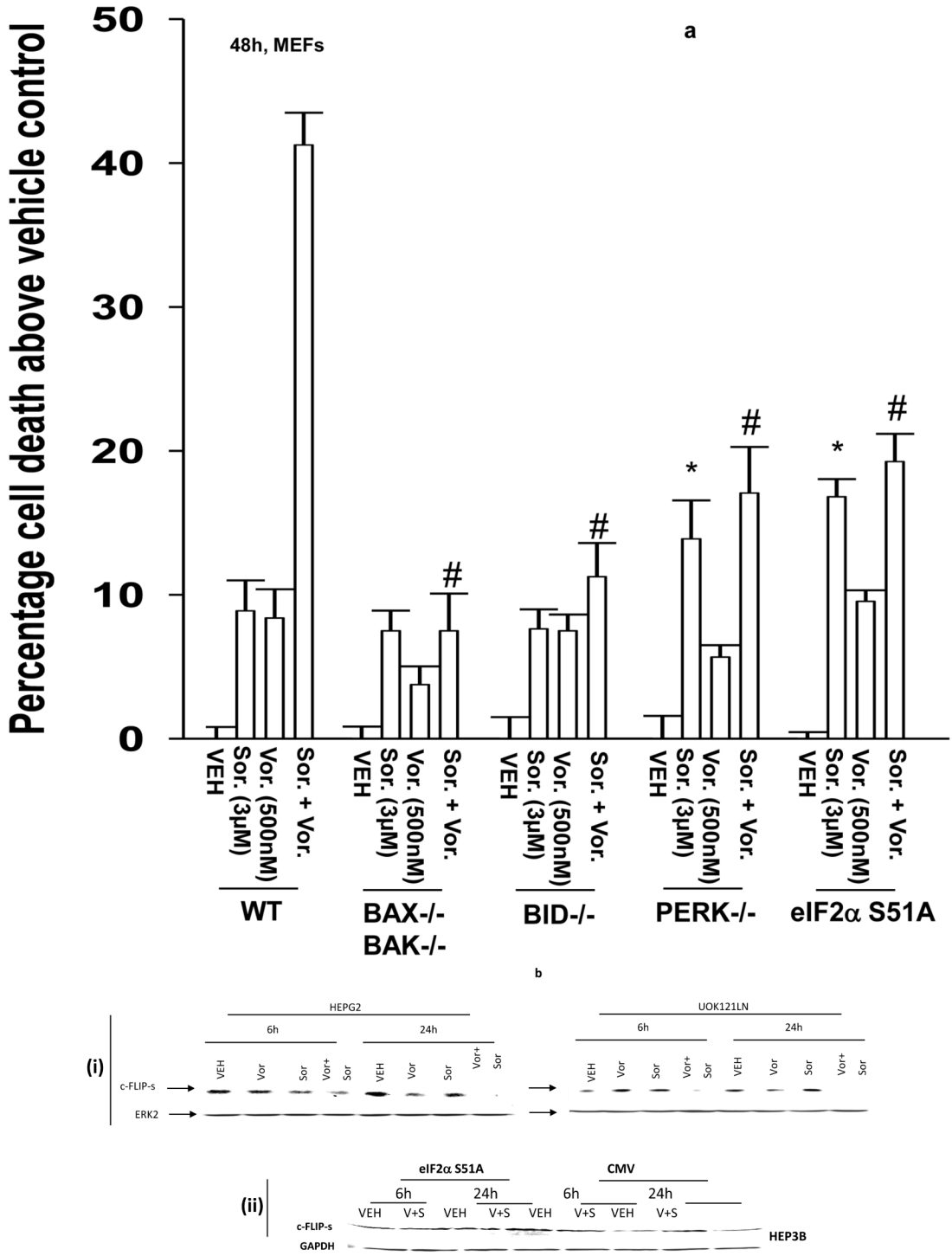

c

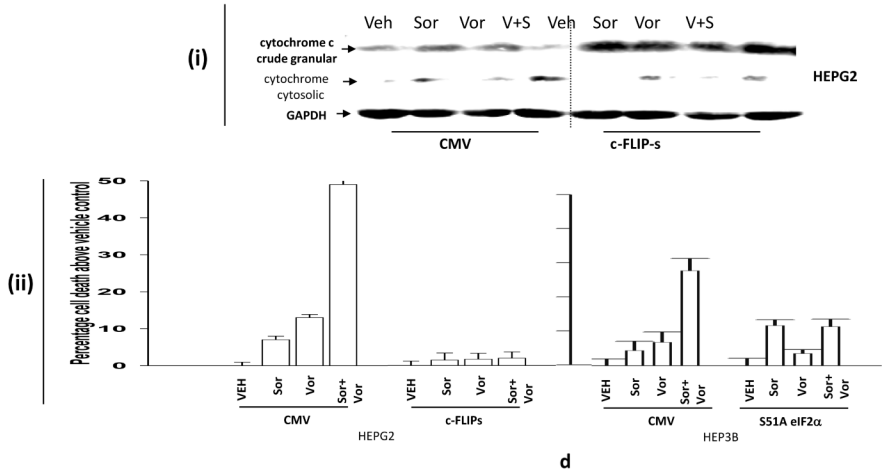

d

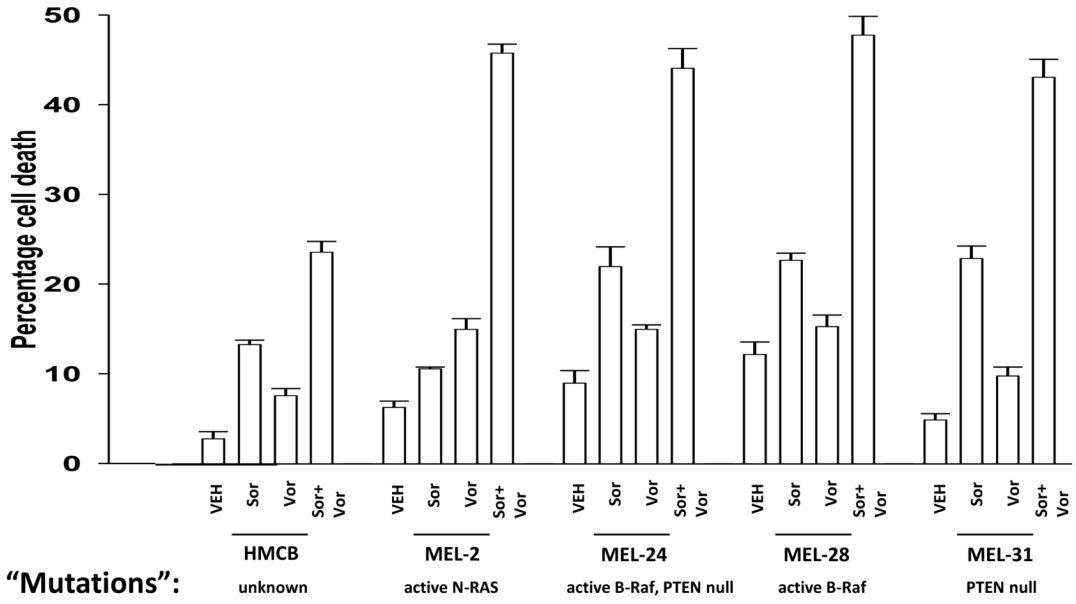

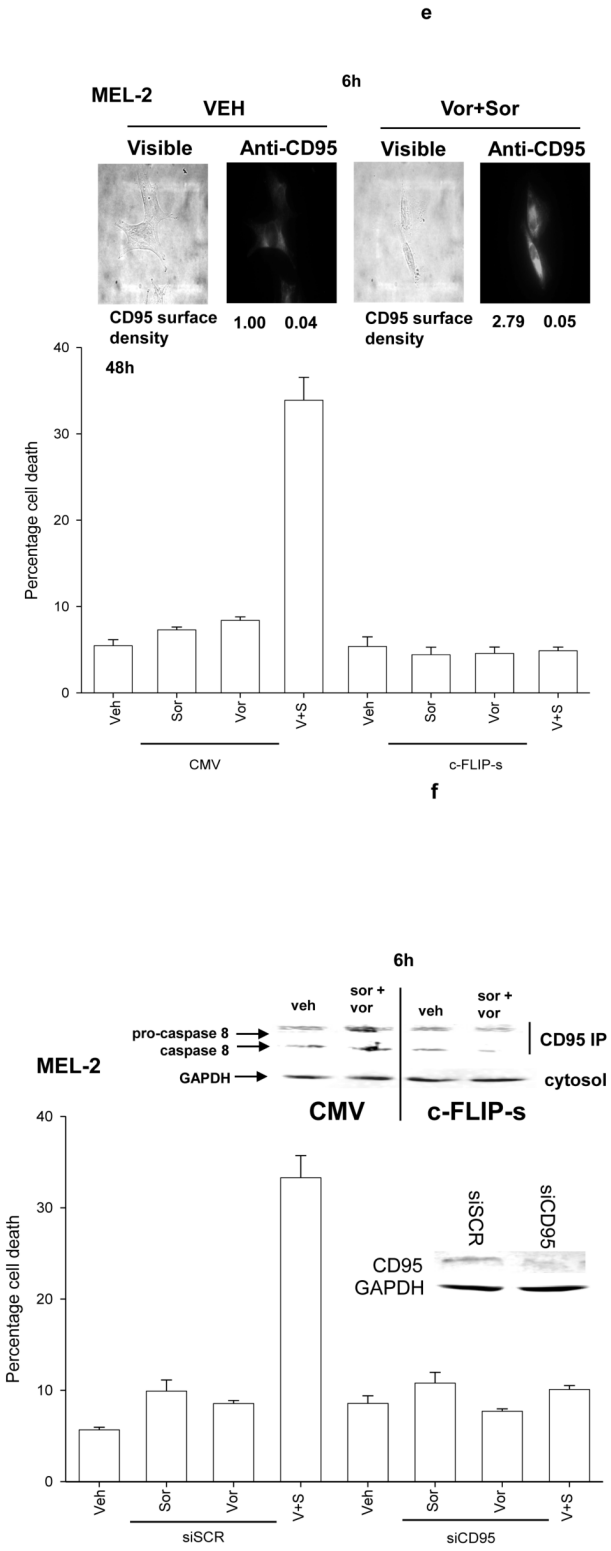

Figure 1. Sorafenib and Vorinostat interact in a synergistic fashion to kill transformed cells via CD95 and PERK-eIF2*α* -induced suppression of c-FLIP-s levels

Panel a. SV40 Large T antigen transformed mouse embryonic fibroblasts lacking expression or with over-expression of various pro- / anti-apoptotic genes were plated in triplicate and treated with vehicle (DMSO), sorafenib (3.0 μM), vorinostat (500 nM) or both sorafenib and vorinostat. Forty eight hours after drug exposure, cells were isolated and viability determined by trypan blue assay. The percentage of trypan blue positive cells ± SEM (n = 3) was determined. # $p < 0.05$ less cell killing than compared to parallel condition in vehicle treatment cells. **Panel b. section (i).** HEPG2 hepatoma and UOK121LN renal cells were plated and treated 24h after plating with vehicle (DMSO), sorafenib (3.0 μM), vorinostat (500 nM) or both sorafenib and vorinostat. Six and 24 hours after drug exposure, cells were isolated and subjected to SDS PAGE followed by immunoblotting to determine the expression of c-FLIP-s and ERK2. Data are from a representative study (n = 3). **section (ii)** HEP3B cells were transfected with either an empty vector plasmid (CMV) or to express dominant negative eIF2α S51A. Twenty four hours after plating, cells were treated with vehicle (DMSO), or with sorafenib (Sor., 3.0 μM) and vorinostat (Vor., 500 nM). Cells were isolated 6h or 24h, as indicated, after drug exposure and the expression of c-FLIP-s and GAPDH determined at each time point. A representative study (n = 2) is shown. **Panel c. section (i)** HEPG2 cells were infected to express empty vector (CMV) or c-FLIP-s. Cells were treated with vehicle (DMSO), sorafenib (3.0 μM), vorinostat (500 nM) or both sorafenib and vorinostat. Twelve hours after drug exposure, cells were isolated and the crude granular and cytosolic fractions isolated. The release of cytochrome c into the cytosolic fraction was determined after SDS PAGE and immunoblotting (n = 2). **section (ii)** HEPG2 cells were infected to express empty vector (CMV) or c-FLIP-s or HEP3B cells transfected to express empty vector or dominant negative eIF2α S51A. Cells were treated with vehicle (DMSO), sorafenib (3.0 μM), vorinostat (500 nM) or both sorafenib and vorinostat. Ninety six hours after drug exposure (HEPG2) or 48h after exposure (HEP3B), cells were isolated and viability determined by trypan blue assay. The percentage of trypan blue positive cells ± SEM (n = 3) was determined. # $p < 0.05$ less cell killing than compared to parallel condition in vehicle treatment cells. **Panel d.** Human malignant melanoma cells were plated in triplicate and treated with vehicle (DMSO), sorafenib (3.0 μM), vorinostat (500 nM) or both sorafenib and vorinostat. After drug exposure (48h), cells were isolated and viability determined by trypan blue assay. The percentage of trypan blue positive cells ± SEM (n = 3) was determined. # $p < 0.05$ less cell killing than compared to parallel condition in vehicle treatment cells. **Panel e.** MEL-2 cells were infected to express empty vector (CMV) or c-FLIP-s. Cells were treated with vehicle (DMSO), sorafenib (3.0 μM), vorinostat (500 nM) or both sorafenib and vorinostat. Forty eight hours after drug exposure, cells were isolated and viability determined by trypan blue assay. The percentage of trypan blue positive cells ± SEM was determined. Data shown are from the mean of 3 independent studies. # $p < 0.05$ less cell killing than compared to parallel condition in vehicle treatment cells. ***upper microscopy:*** MEL-2 cells were plated on glass slides and treated 24h after plating with vehicle (DMSO) or with sorafenib (3.0 μM) and vorinostat (500 nM). Six hours after drug exposure, cells were fixed in situ. Fixed cells were blocked then incubated with an anti-CD95 antibody. Cells were then incubated with a 488nm-tagged fluorescent secondary antibody. Cells were washed, cover-slipped and analyzed on a fluorescent microscope (X100 mag.). The intensity of CD95 staining was determined at 50 random points per cell for a total of 5 cells ± SEM (n = 3 separate studies). **Panel f.** MEL-2 cells were transfected with a non-specific scrambled control (siSCR) siRNA molecule or a molecule to knock down the expression of CD95 according to the manufacturer's instructions. Cells were treated 24h after transfection with vehicle (DMSO), sorafenib (3.0 μM), vorinostat (500 nM) or both sorafenib and vorinostat. Ninety six hours after drug exposure, cells were isolated and viability determined by trypan blue assay. The percentage of trypan blue positive cells ± SEM was determined. Data shown are from the mean of 3 independent studies. # $p < 0.05$ less cell killing than compared to parallel condition in vehicle treatment cells. ***upper blotting:*** MEL-2 cells infected to express empty vector (CMV) or c-FLIP-s and treated 24h after infection with vehicle (DMSO) or with sorafenib (3.0 μM) and vorinostat (500 nM). Cells were isolated 6h

after sorafenib and vorinostat exposure and CD95 immunoprecipitated from the cell lysate. SDS PAGE followed by immunoblotting of CD95 immunoprecipitates was performed to determine the association of pro-caspase 8 and caspase 8 with CD95. Data are from a representative study (n = 3).

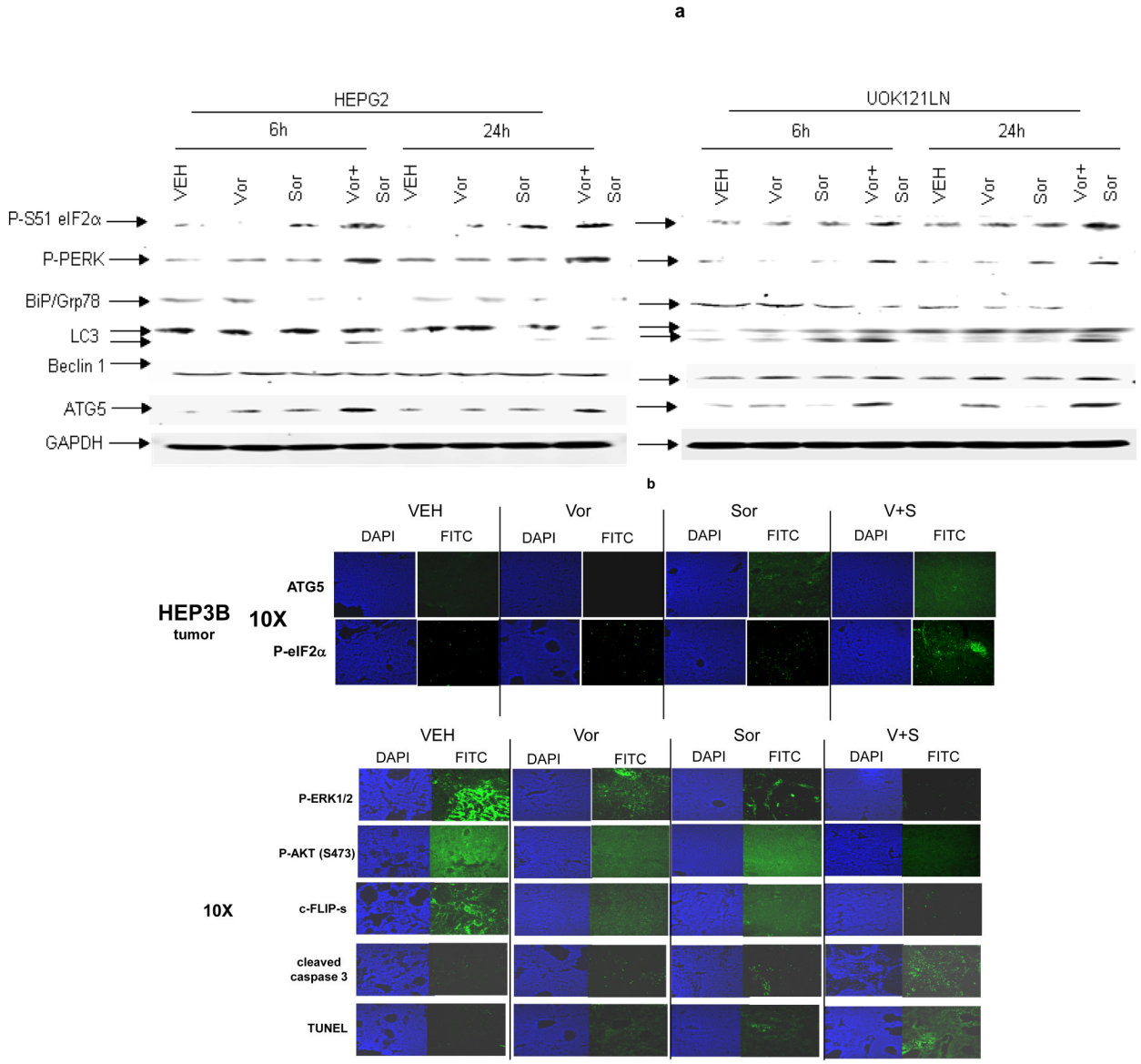

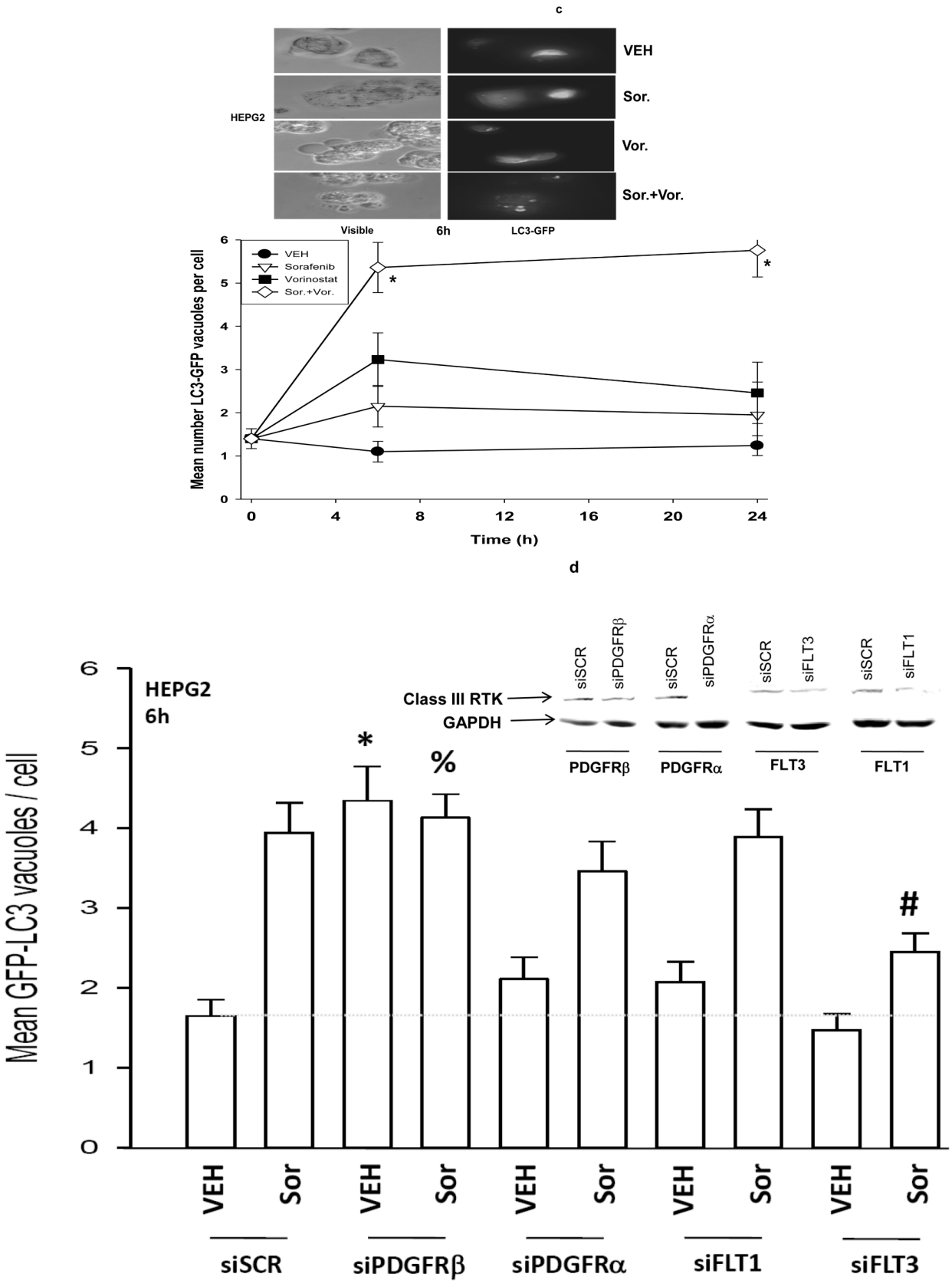

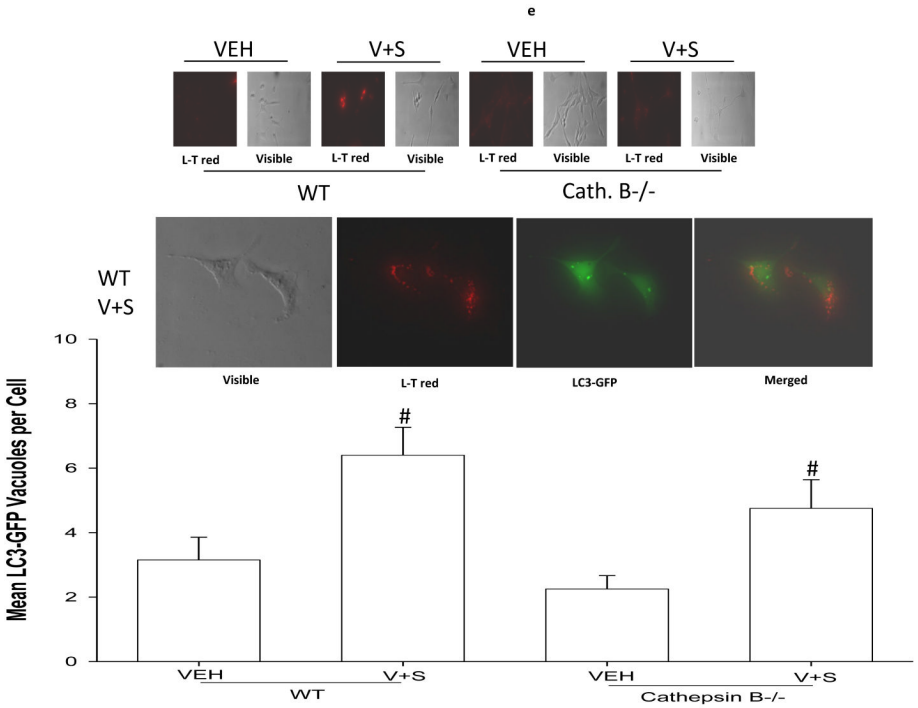

Figure 2. Sorafenib and Vorinostat interact to cause tumor cell death in vivo; sorafenib and vorinostat promote PERK activation and the induction of autophagy

Panel a. HEPG2 and UOK121LN cells were plated and treated 24h after plating with vehicle (DMSO), sorafenib (3.0 μM), vorinostat (500 nM) or both sorafenib and vorinostat. Six and 24 hours after drug exposure, cells were isolated and subjected to SDS PAGE followed by immunoblotting to determine the expression of BiP/Grp78, LC3, Beclin1, ATG5 and GAPDH and the phosphorylation of eIF2α S51 and PERK T981. **Panel b.** HEP3B cells were injected (10^7) into the flanks of athymic mice and tumors permitted to form. The tumor take-rate was approximately 20%. Tumors were permitted to grow to ~150 mm^3 after which time tumors were segregated based on volume into relatively normalized groups. Animals / tumors in triplicate were subjected to vehicle / drug administration by oral gavage once daily for three consecutive days. BAY 54-9085 was administered at a dose of 45 mg/kg. Vorinostat was administered at a dose of 25 mg/kg. Twelve hours after the final gavage dosing, the animals were humanely sacrificed, the tumors were removed and sectioned. The tumor was subjected for immunohistochemical analyses to determine eIF2α phosphorylation, ERK1/2 phosphorylation, AKT (S473) phosphorylation, and the expression of ATG5, c-FLIP-s, MCL-1, caspase 3 cleavage status, and TUNEL positivity (n = 2 separate experiments). **Panel c.** HEPG2 cells were transfected with an LC3-GFP construct. Twenty four hours after transfection, cells were treated with vehicle (DMSO), sorafenib (3.0 μM), vorinostat (500 nM) or both sorafenib and vorinostat. Six and 24 hours after drug exposure, cells were visualized at 40X using an Axiovert 200 fluorescent microscope under fluorescent light on the Zeiss Axiovert 200 microscope using the FITC filter, and visible light. The mean number of autophagic vesicles per cell from random fields of 40 cells were counted (± SEM, n = 3). The pictorial data shown is from a representative experiment (n = 3). **Panel d.** HEPG2 cells were transfected with an LC3-GFP construct and simultaneously transfected with either a scrambled siRNA (siSCR) or validated siRNA molecules to knock down the expression of the PDGFRα, PDGFRβ, FLT1 or FLT3. Twenty four hours after transfection, cells were treated with vehicle (DMSO) or sorafenib (6.0 μM) for 6h. cells were visualized at 40X using an Axiovert 200 fluorescent microscope under fluorescent light on the Zeiss Axiovert 200 microscope using the FITC filter, and visible light. The mean number of autophagic vesicles

per cell from random fields of 50 cells were counted (± SEM, n = 5). *$p < 0.05$ greater than vehicle control; #$p < 0.05$ less than corresponding value in siSCR treated cells; %$p > 0.05$ greater / less than corresponding value in siSCR treated cells. **Panel e.** Wild type and cathepsin B -/- immortalized fibroblasts were transfected with an LC3-GFP construct. Twenty four hours after transfection, cells were treated with vehicle (DMSO), sorafenib (3.0 μM), vorinostat (500 nM) or both sorafenib and vorinostat. Six hours after drug exposure, cells were visualized at 40X under fluorescent light on the Zeiss Axiovert 200 microscope using the FITC and Rhodamine filters, as well as visible light. The mean number of autophagic vesicles per cell from random fields of 40 cells were counted (± SEM, n = 2). The upper pictorial data from parallel treated cells stained with lysotracker red (see ref [29]; n = 40 per slide examined) and examined under the rhodamine filter are from a representative experiment (n = 2). Cells were merged in Adobe Photoshop CS2 to examine LC3-GFP vesicle and lysotracker red staining co-localization.

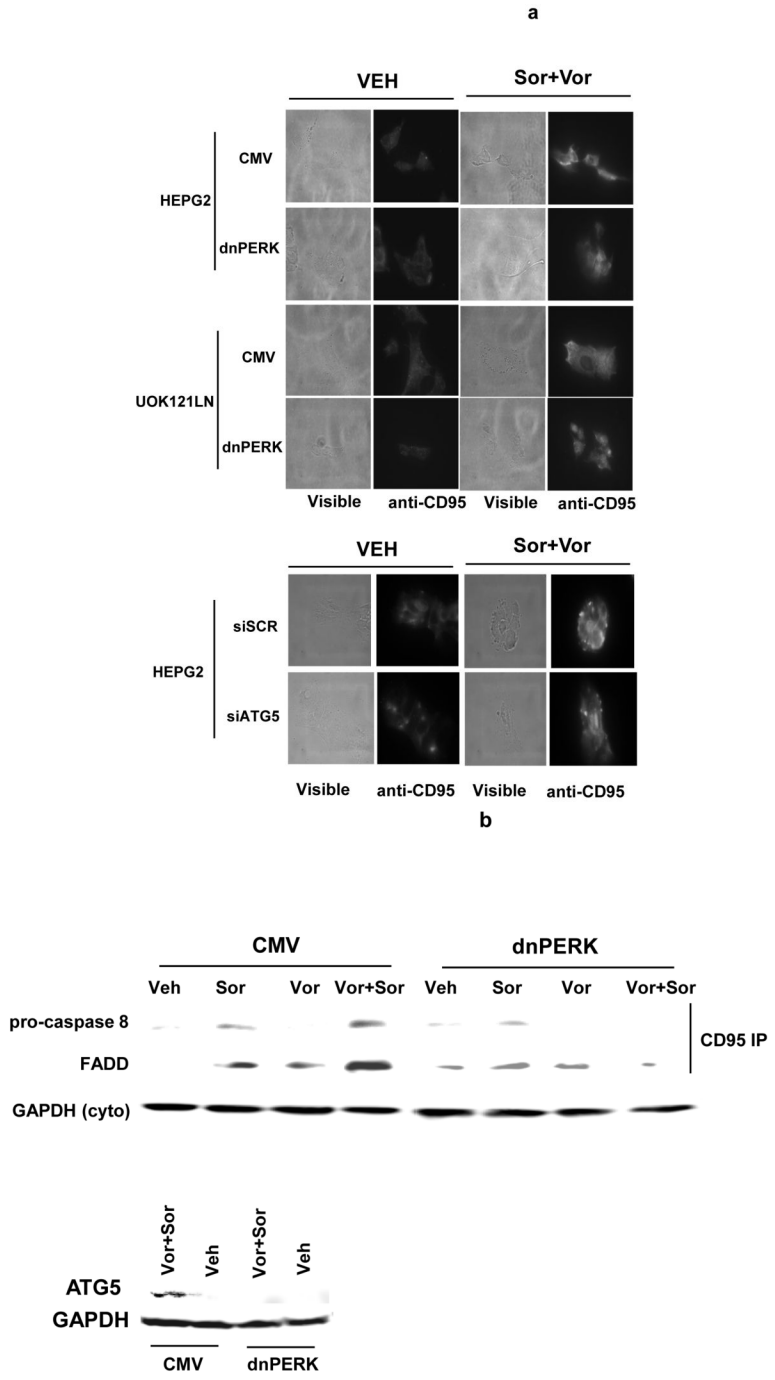

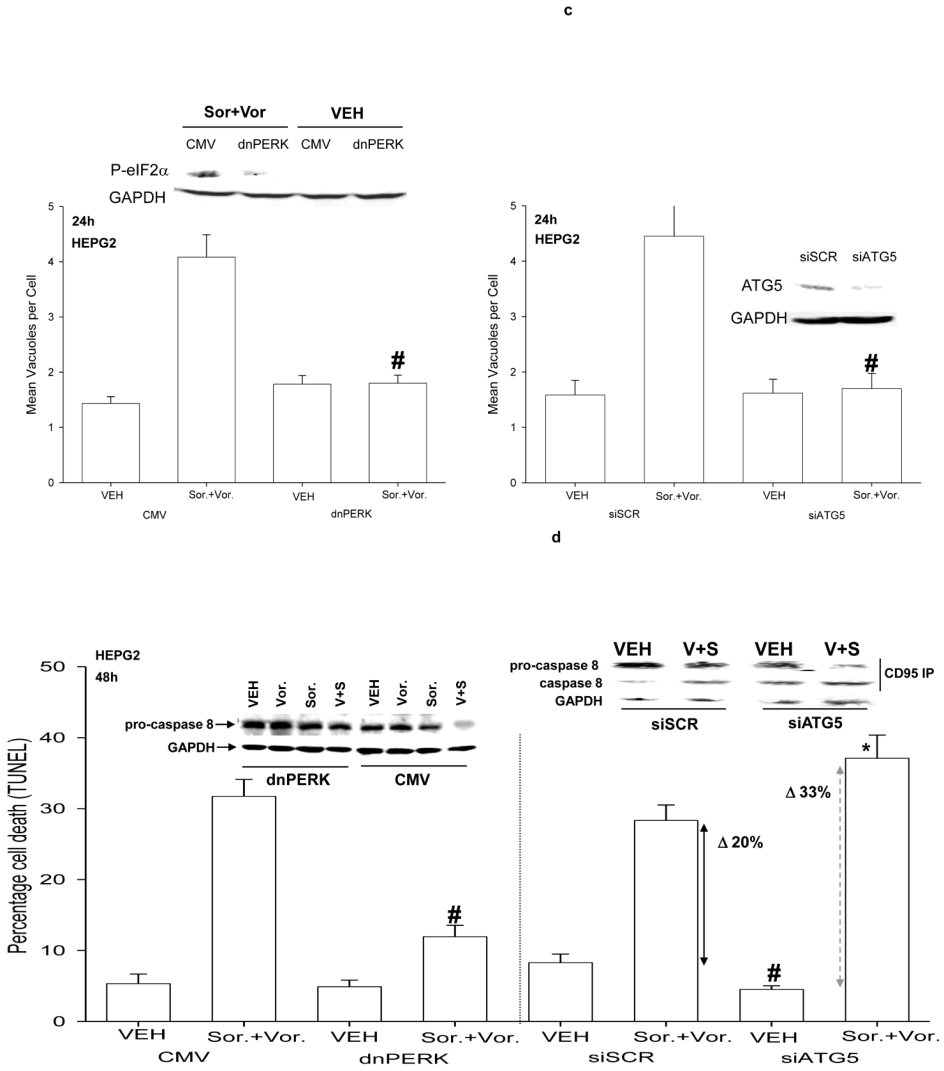

Figure 3. Sorafenib and vorinostat treatment modulates DISC formation, ER stress signaling and autophagy via CD95-PERK signaling

Panel a. HEPG2 and UOK121LN cells were plated on glass slides and either transfected to express dominant negative PERK or transfected to knock down expression of ATG5. Cells were treated 24h after transfection with vehicle (DMSO) or with sorafenib (3.0 μM) and vorinostat (500 nM). Six hours after drug exposure, cells were fixed in situ. Fixed cells were blocked then incubated with an anti-CD95 antibody. Cells were then incubated with a 488nm-tagged fluorescent secondary antibody. Cells were washed, cover-slipped and analyzed on a fluorescent microscope (X100 magnification). The intensity of CD95 staining was determined at 50 random points per cell for a total of 5 cells ± SEM (n = 3 separate studies). **Panel b. Upper panel:** HEPG2 cells transfected to express empty vector (CMV) or dominant negative PERK (dnPERK) and treated 24h after infection with vehicle (DMSO) or with sorafenib (3.0 μM) and/or vorinostat (500 nM). Cells were isolated 6h after sorafenib and vorinostat exposure and CD95 immunoprecipitated from the cell lysate. SDS PAGE followed by immunoblotting of CD95 immunoprecipitates was performed to determine the association of pro-caspase 8 and caspase 8 with CD95. Data are from a representative study (n = 2). **Lower panel:** HEPG2 cells transfected to express empty vector (CMV) or dominant negative PERK (dnPERK) and treated 24h after infection with vehicle (DMSO) or with sorafenib (3.0 μM) and vorinostat (500 nM).

Cells were isolated 24h after sorafenib and vorinostat exposure and the expression of ATG5 and GAPDH determined by SDS PAGE followed by immunoblotting (a representative, n = 2). **Panel c.** HEPG2 cells were transfected with an LC3-GFP construct and co-transfected either to express dominant negative PERK or co-transfected to knock down expression of ATG5. Twenty four hours after transfection, cells were treated with vehicle (DMSO), sorafenib (3.0 μM), vorinostat (500 nM) or both sorafenib and vorinostat. Twenty four hours after drug exposure, cells were visualized at 40X using an Axiovert 200 fluorescent microscope under fluorescent light on the Zeiss Axiovert 200 microscope using the FITC filter. The mean number of autophagic vesicles per cell from random fields of 40 cells were counted (± SEM, n = 3). The upper immunoblotting sections are presented for control purposes to demonstrate that expression of dominant negative PERK blocked drug-induced phosphorylation of eIF2α and that the siRNA to ATG5 knocked down ATG5 expression (n = 2). **Panel d. Graphical panel:** HEPG2 cells were plated in triplicate and either transfected to express dominant negative PERK or transfected to knock down expression of ATG5. Cells were treated 24h after transfection with vehicle (DMSO) or with sorafenib (3.0 μM) and vorinostat (500 nM). Forty eight hours after drug exposure cells were isolated and cell viability determined by TUNEL assay (± SEM, n = 2 independent assays). **Upper inset blot to left:** in cells transfected with dominant negative PERK the ability of vorinostat and sorafenib to promote pro-caspase 8 cleavage was determined 48h after drug exposure. **Upper inset blot to right:** HEPG2 cells were plated in triplicate and transfected to knock down expression of ATG5. Cells were treated 24h after transfection with vehicle (DMSO) or with sorafenib (3.0 μM) and vorinostat (500 nM). Six h after drug exposure cells were lysed and CD95 immunoprecipitated from the cell lysate. SDS PAGE followed by immunoblotting of CD95 immunoprecipitates was performed to determine the association of pro-caspase 8 and caspase 8 with CD95. Data are from a representative study (n = 3).

a

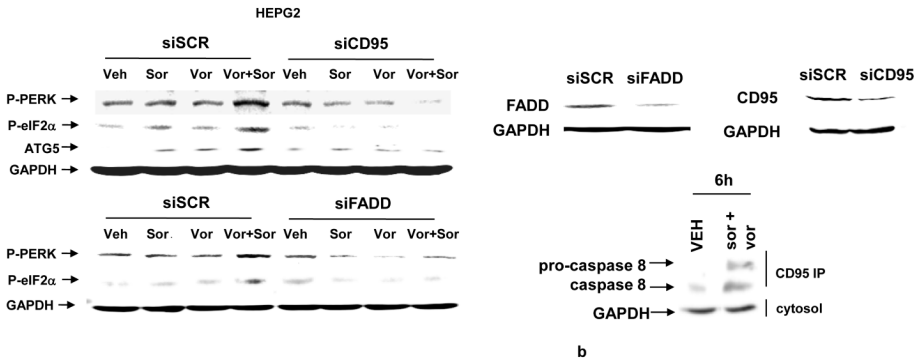

b

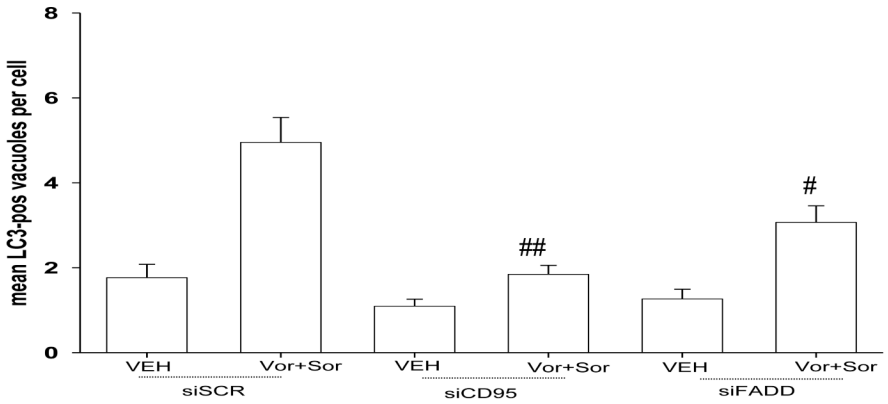

c

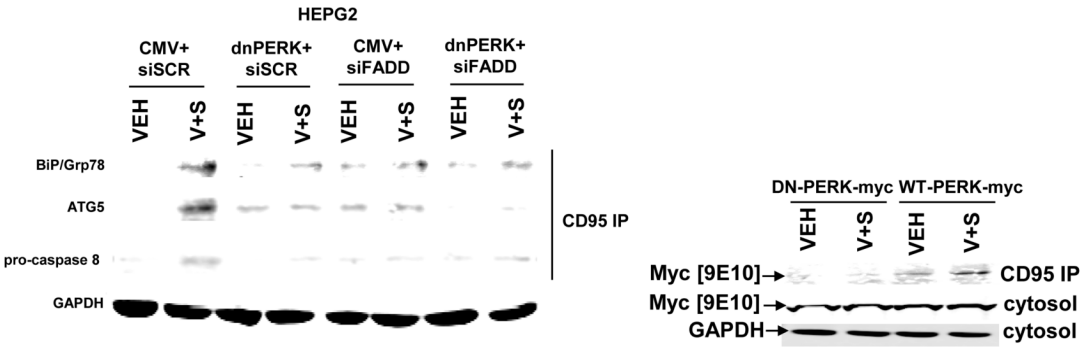

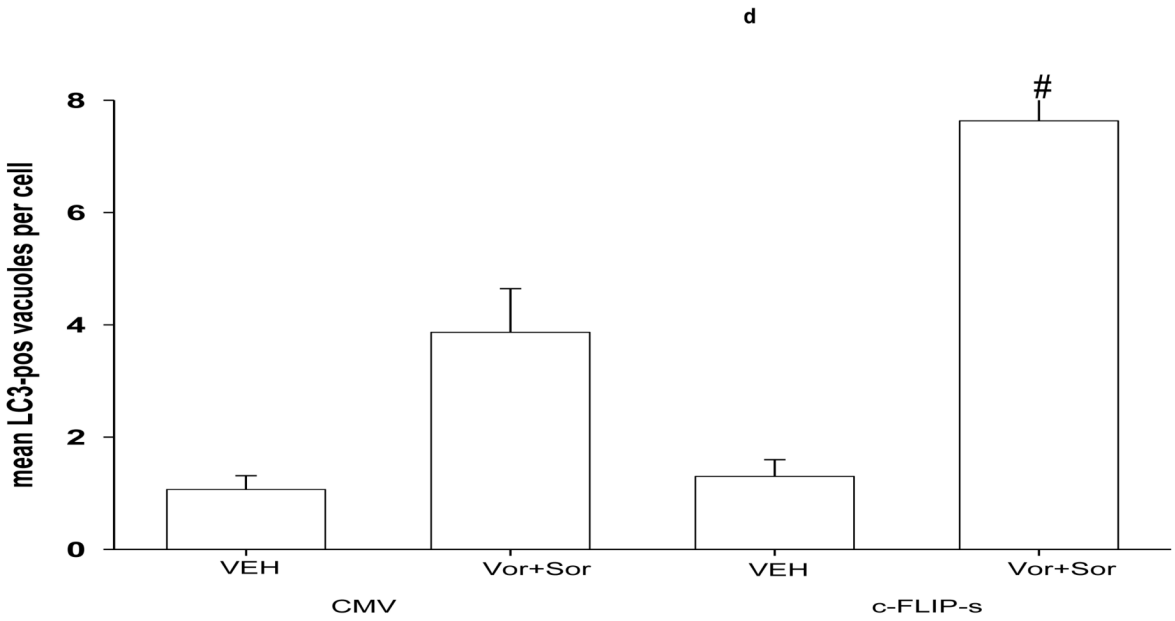

Figure 4. Sorafenib and vorinostat -induced activation of PERK is CD95-dependent

Panel a. HEPG2 cells were transfected to knock down expression of CD95 or FADD. Cells were treated 24h after transfection with vehicle (DMSO), sorafenib (3.0 μM), vorinostat (500 nM) or both sorafenib and vorinostat. Six hours after drug exposure, cells were isolated and subjected to SDS PAGE followed by immunoblotting to determine the expression of FADD, CD95, ATG5 and GAPDH, and in parallel the phosphorylation of PERK and eIF2α. Data are from a representative study (n = 3). *Lower right:* In parallel as a positive control, 6h after drug exposure, CD95 was immunoprecipitated and the formation of a DISC complex containing pro-caspase 8 demonstrated. **Panel b.** HEPG2 cells were plated on glass slides and transfected with a non-specific scrambled control (siSCR) siRNA molecule, or molecules to knock down the expression of CD95 or FADD, according to the manufacturer's instructions. In parallel, cells were transfected with a construct to express LC3-GFP. Cells were treated 24h after transfection with vehicle (DMSO) or with sorafenib (3.0 μM) and vorinostat (500 nM). Twenty four hours after drug exposure, cells were visualized at 40X using an Axiovert 200 fluorescent microscope under fluorescent light on the Zeiss Axiovert 200 microscope using the FITC filter. The mean number of autophagic vesicles per cell from random fields of 40 cells were counted (± SEM, n = 3). **Panel c.** ***Left blotting section:*** HEPG2 cells were transfected to express dominant negative PERK or to knock down expression of FADD. Cells were treated 24h after transfection with vehicle (DMSO), sorafenib (3.0 μM), vorinostat (500 nM) or both sorafenib and vorinostat. Six hours after drug exposure, cells were isolated CD95 was immunoprecipitated and the formation of a DISC complex containing pro-caspase 8 demonstrated. The association of other proteins: BiP/Grp78 and ATG5 was determined. The cytosolic fraction was analyzed for GAPDH expression (n = 2). ***Right blotting section:*** HEPG2 cells were transfected with either MYC-tagged wild type PERK or MYC-tagged dominant negative PERK. Cells were treated 24h after transfection with vehicle (DMSO) or with sorafenib (3.0 μM) and vorinostat (500 nM). Six hours after drug exposure, cells were isolated, CD95 was immunoprecipitated and the association of PERK proteins with CD95 determined by immunoblotting the MYC tag using an anti-Myc 9E10 antibody (a representative study, n = 2 is shown). **Panel d.** HEPG2 cells were plated on glass slides and infected with a recombinant adenovirus to express c-FLIP-s. In parallel, cells were transfected with a construct to express LC3-GFP. Cells were treated 24h after transfection with vehicle (DMSO) or with sorafenib (3.0 μM) and vorinostat (500 nM). Twenty four hours after drug exposure, cells were visualized

at 40X using an Axiovert 200 fluorescent microscope under fluorescent light on the Zeiss Axiovert 200 microscope using the FITC filter. The mean number of autophagic vesicles per cell from random fields of 40 cells were counted (± SEM, n = 2).

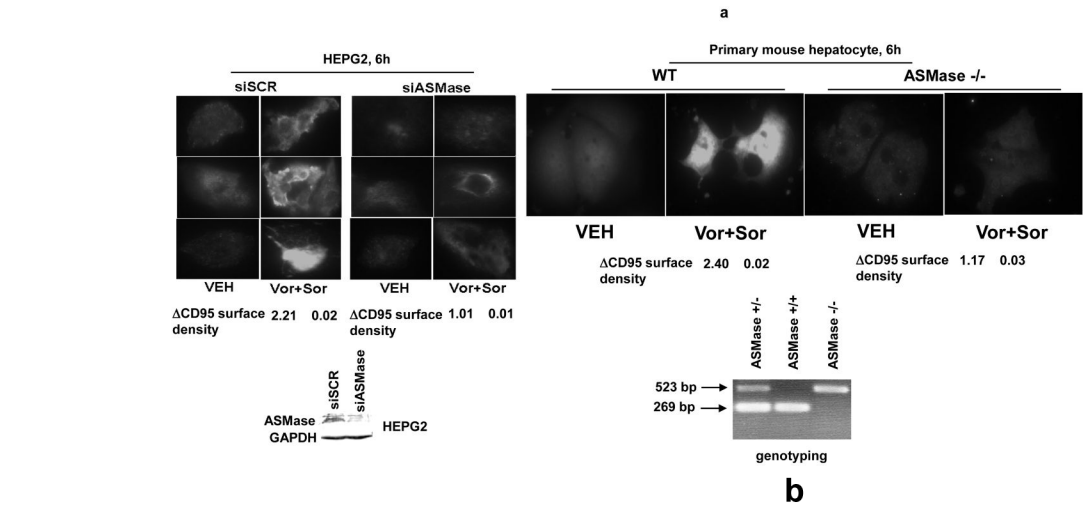

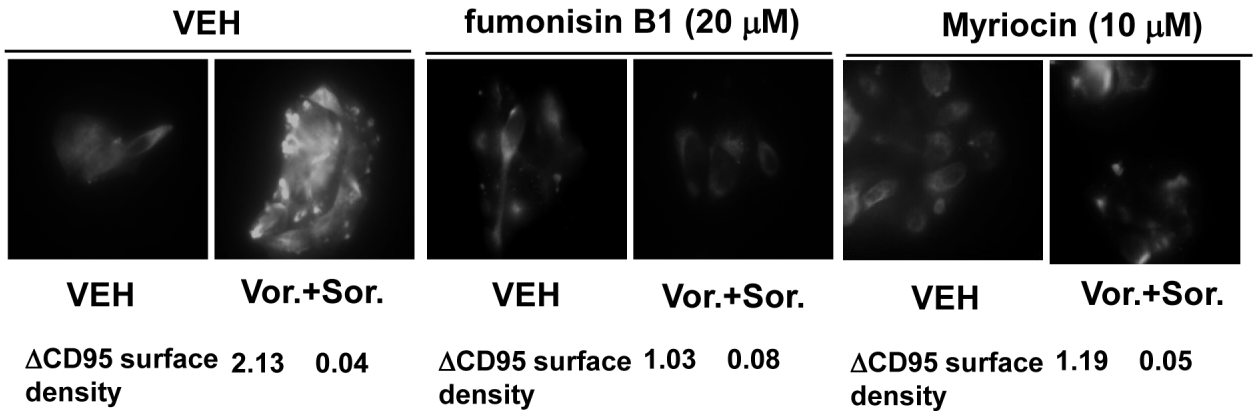

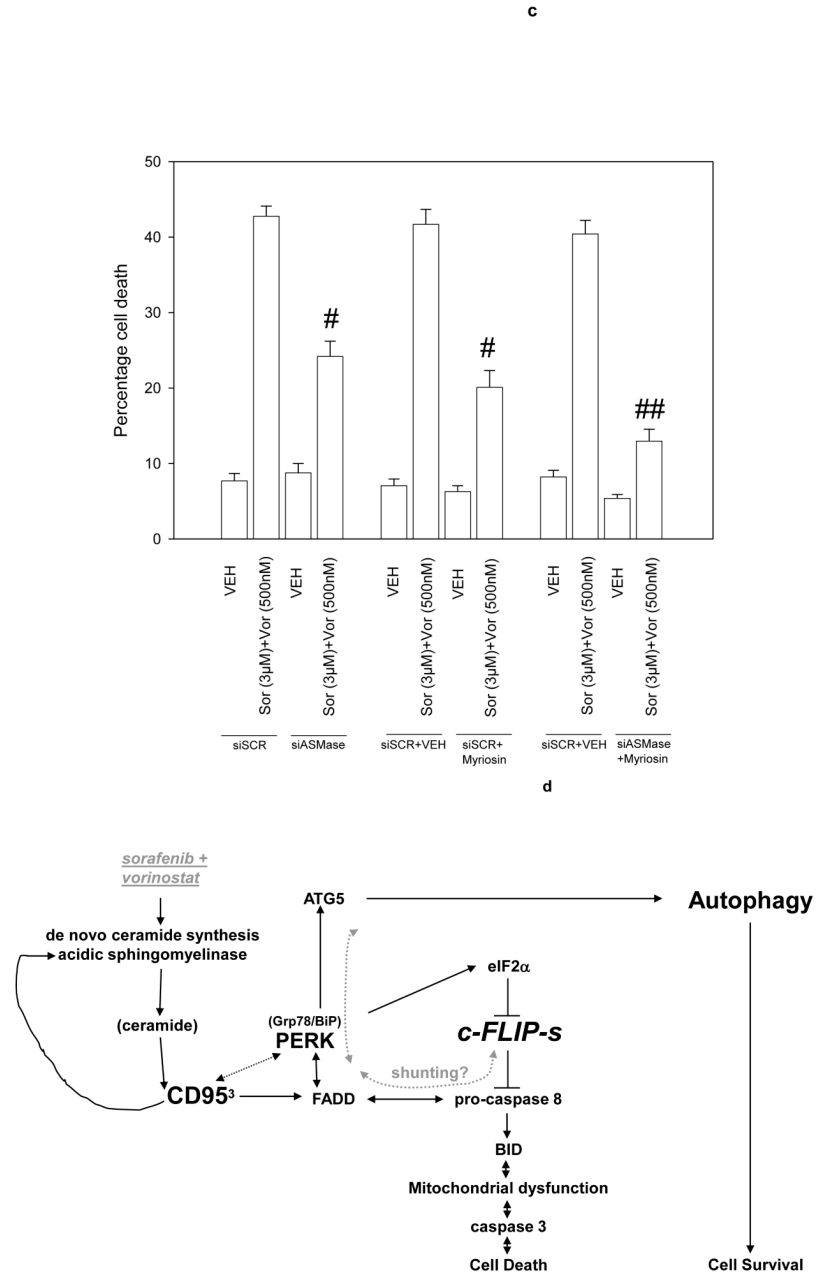

Figure 5. Sorafenib and vorinostat -induced activation of CD95 is acidic sphingomyelinase dependent

Panel a. HEPG2 cells were plated on glass slides and were transfected with as siRNA to knock down acidic sphingomyelinase expression (siASMase). Cells were treated 24h after plating with vehicle (DMSO) or with sorafenib (3.0 μM) and vorinostat (500 nM). Six hours after drug exposure, cells were fixed in situ. Fixed cells were blocked then incubated with an anti-CD95 antibody. Cells were then incubated with a 488nm-tagged fluorescent secondary antibody. Cells were analyzed on a fluorescent microscope (X100 magnification). The intensity of CD95 staining was determined at 50 random points per cell for a total of 5 cells ± SEM (n = 3 separate studies). **Panel b.** Primary mouse hepatocytes were isolated as described in reference (11) and were plated on collage type I coated glass slides. Cells were cultured for 24h after isolation followed by treatment with vehicle (VEH, DMSO) or with sorafenib (3.0 μM) and vorinostat

(500 nM). Six hours after drug exposure, cells were fixed in situ. Fixed cells were blocked then incubated with an anti-CD95 antibody. Cells were then incubated with a 488nm-tagged fluorescent secondary antibody. Cells were analyzed on a fluorescent microscope (X100 magnification). The intensity of CD95 staining was determined at 50 random points per cell for a total of 5 cells ± SEM (n = 2 separate studies). **Panel c.** In parallel to the transfection (siSCR and siASMase); de novo pathway drug inhibitor siSCR transfection plus (VEH and myriosin; Myr., 10 μM); or inhibition of both pathways simultaneously, as indicated, for the treatments used cells in *Panels A and B*, cells were incubated for 48h after vehicle (VEH, DMSO) or with sorafenib (3.0 μM) and vorinostat (500 nM). Forty eight hours after drug exposure cells were isolated and cell viability determined by TUNEL assay (± SEM, n = 2 independent assays). **Panel d.** Putative mechanisms of vorinostat and sorafenib action in epithelial tumor cells. Vorinostat and sorafenib increase ceramide levels. Ceramide permits CD95 plasma membrane localization and activation. CD95 activation leads to the induction of at least three immediate downstream survival regulatory signals: activation of pro-caspase 8 (death); activation of PERK-eIF2α-ER stress (death); activation of PERK-ATG5-autophagy (survival). Over-expression of c-FLIP-s forces the CD95 signal away from cell killing towards increased autophagy (survival). Knock down of ATG5 forces the CD95 signal away from autophagy and towards increased cell killing (caspase 8 cleavage).

Table 1

The sorafenib synergizes with vorinostat to kill melanoma cells that is abolished by overexpression of c-FLIP-s

Melanoma (MEL-2) and NSCLC (A549) cells were infected 12h after plating at an approximate multiplicity of infection of 50 with either a control empty vector recombinant adenovirus (CMV) or a recombinant virus to express the caspase 8 inhibitor c-FLIP-s. Twenty four hours after infection, infected cells were plated as single cells (250-1500 cells/well) in sextuplicate and 12h after this plating the infected cells were treated with vehicle (VEH, DMSO), sorafenib (Sor., 3.0-6.0 μM) or vorinostat (Vor. 250-500 nM), or with both drugs combined, as indicated at a fixed concentration ratio to perform median dose effect analyses for the determination of synergy. Forty eight hours after drug exposure, the media was changed and cells cultured in drug free media for an additional 10-14 days. Cells were fixed, stained with crystal violet and colonies of > 50 cells / colony counted. Colony formation data were entered into the Calcusyn program and combination index (CI) values determined. A CI value of less than 1.00 indicates synergy

MEL-2				**A549**			
CMV				**CMV**			
Sorafenib (*μ*M)	**Vorinostat (*μ*M)**	**Fa**	**CI**	**Sorafenib (μM)**	**Vorinostat (μM)**	**Fa**	**CI**
3.0	0.250	0.32	0.517	3.0	0.250	0.25	0.412
4.5	0.375	0.36	0.594	4.5	0.375	0.31	0.508
6.0	0.500	0.44	0.653	6.0	0.500	0.38	0.561

c-FLIP-s				**c-FLIP-s**			
Sorafenib (*μ*M)	**Vorinostat (*μ*M)**	**Fa**	**CI**	**Sorafenib (μM)**	**Vorinostat (μM)**	**Fa**	**CI**
3	0.25	0.09	1.072	3.0	0.25	0.09	0.830
4.5	0.375	0.12	1.336	4.5	0.375	0.11	0.987
6	0.5	0.24	1.118	6.0	0.5	0.13	1.081

Table 2

Sorafenib and vorinostat rapidly modulate the levels of ceramide and sphingosine lipids in HEPG2 cells

Parallel sets of HEPG2 cells from Figure 5 ***panels A and B*** were scraped into PBS 3h after either vehicle or vorinostat and sorafenib exposure and isolated by centrifugation followed by freezing at -80°C. Lipids were isolated from the cells and ceramide and sphingosine isoforms analyzed by tandem mass spectrometry according to Bielawski et al. (49). Data are presented as concentration value ***pmole each lipid / total sample***. *Upper section:* For ASMase knock down data are the mean of seven determinations ± SEM from three independent experiments. Abbreviations: Cer: ceramide; dh: dihydro; Sph: sphingosine; P: phosphate; siSCR: scramble siRNA; siASMase: siRNA to knock down acidic sphingomyelinase expression. Values marked with an asterisk (*) indicate the difference between Vehicle (VEH) treated and vorinostat and sorafenib (V+S) treated samples had a significance of at least $p < 0.05$. Values marked with a hatch mark (#) indicate the difference between siSCR and siASMase vehicle (i.e. basal levels) treated samples had a significance of at least $p < 0.05$. *Lower section:* For fumonisin B1 inhibitor use, data are the mean of six determinations ± SEM from two independent experiments. Abbreviations: Fum. B1: Fumonisin B1. Values marked with an asterisk (*) indicate the difference between Vehicle (VEH) treated and vorinostat and sorafenib (V+S) treated samples had a significance of at least $p < 0.05$. Values marked with a hatch mark (#) indicate the difference between V+S treated samples in VEH and Fum. B1 treated samples that had a significant reduction of at least $p < 0.05$

	Cer 14	Cer 16	Dh Cer 12	Dh Cer 14	Dh Cer 16	Dh Cer 18	Dh Cer 20	Dh Cer 22	Dh Cer 22:1	Dh Cer 24	Dh Cer 24:1	Dh Cer 26	Dh Cer 26:1	Dh Sph	Dh Sph -1-P	Sph	Sph -1-P
	8.1	41.8	0.09	4.1	16.8	4.0	8.8	5.0	13.1	10.7	5.3	0.9	0.4	1.19	0.31	3.7	0.7
	14.7 *	61.9 *	0.44 *	18.4 *	81.3 *	20.0 *	34.2 *	22.8 *	34.4 *	37.1 *	31.8 *	1.7 *	0.7 *	1.71 *	0.19 *	3.8	0.8
H	11.4 #	71.4 #	0.11	3.7	17.5	3.8	7.7	5.2	15.3	7.4	3.9	0.9	0.5	1.60	0.24	3.3	1.1
S	13.1	74.4	0.51 *	16.9 *	99.0 *	15.5 *	24.0 *	25.3 *	29.7 *	39.7 *	30.3 *	1.9 *	1.0 *	1.59	0.25	3.8	1.3

	Cer 14	Cer 16	Dh Cer 12	Dh Cer 14	Dh Cer 16	Dh Cer 18	Dh Cer 20	Dh Cer 22	Dh Cer 22:1	Dh Cer 24	Dh Cer 24:1	Dh Cer 26	Dh Cer 26:1	Dh Sph	Dh Sph -1-P	Sph	Sph -1-P
	7.9	38.6	0.09	1.3	6.6	1.3	2.0	3.1	6.6	2.8	1.1	0.7	0.2	0.6	0.9	5.8	0.3
	12.5 *	55.9 *	0.40 *	11.7 *	61.3 *	9.5 *	14.3 *	17.9 *	10.0 *	24.5 *	17.9 *	1.3 *	0.3	0.8	0.6	7.3	0.5
	6.4	39.1	0.10	2.1	8.0	1.6	3.0	4.1	8.9	3.9	1.5	0.9	0.3	0.8	0.9	8.6	0.6
	11.9 *	55.4 *	0.21 #	9.7 #*	52.0 #*	8.1 *	11.7 #*	16.9 *	9.0 #	21.4 *	16.0 *	0.9 #	0.2	0.9	0.8	8.3	0.8